

The Emergence of Lobsters: Phylogenetic Relationships, Morphological Evolution and Divergence Time Comparisons of an Ancient Group (Decapoda: Achelata, Astacidea, Glypheidea, Polychelida)

HEATHER D. BRACKEN-GRISSOM^{1,*}, SHANE T. AHYONG^{2,3}, RICHARD D. WILKINSON⁴, RODNEY M. FELDMANN⁵, CARRIE E. SCHWEITZER⁶, JESSE W. BREINHOLT⁷, MATTHEW BENDALL⁸, FERRAN PALERO⁹, TIN-YAM CHAN¹⁰, DARRYL L. FELDER¹¹, RAFAEL ROBLES¹², KA-HOU CHU¹³, LING-MING TSANG^{10,13}, DOHYUP KIM⁸, JOEL W. MARTIN¹⁴, AND KEITH A. CRANDALL¹⁵

¹Department of Biology, Florida International University, 3000 NE 151st Street, North Miami, FL 33181, USA;

²Australian Museum, 6 College Street, Sydney, NSW 2010, Australia;

³University of New South Wales, Kensington, NSW 2052, Australia;

⁴School of Mathematical Sciences, University of Nottingham, Nottingham, UK;

⁵Department of Geology, Kent State University, Kent, OH 44242, USA;

⁶Kent State University at Stark, 6000 Frank Avenue NW, North Canton, OH 44720, USA;

⁷Florida Museum of Natural History, University of Florida, Gainesville, FL 32611, USA;

⁸Brigham Young University, 401 WIDB, Provo, UT 84606, USA;

⁹Unitat Mixta Genòmica i Salut CSISP-UV, Institut Cavanilles Universitat de Valencia, C/Catedrático Jose Beltran 2, 46980 Paterna, Spain;

¹⁰Institute of Marine Biology and Center of Excellence for Marine Bioenvironment and Biotechnology, National Taiwan Ocean University, Keelung 20224, Taiwan, R.O.C.;

¹¹Department of Biology, University of Louisiana at Lafayette, Lafayette, LA 70504, USA;

¹²Laboratory of Bioecology and Crustacean Systematics, Department of Biology, FFCLRP, University of São Paulo (USP), Ave. Bandeirantes 3900, CEP 14040–901, Ribeirão Preto, SP Brazil;

¹³School of Life Sciences, The Chinese University of Hong Kong, Shatin, Hong Kong;

¹⁴Natural History Museum of Los Angeles County, Los Angeles, CA 90007, USA;

¹⁵George Washington University, Computational Biology Institute, Ashburn, VA 20147, USA;

*Correspondence to be sent to: Department of Biology, Florida International University, 3000 NE 151st St, North Miami, FL 33181, USA; E-mail: hbracken@fiu.edu.

Received 28 June 2013; reviews returned 15 October 2013; accepted 10 February 2014

Associate Editor: Thomas Near

Abstract.—Lobsters are a ubiquitous and economically important group of decapod crustaceans that include the infraorders Polychelida, Glypheidea, Astacidea and Achelata. They include familiar forms such as the spiny, slipper, clawed lobsters and crayfish and unfamiliar forms such as the deep-sea and “living fossil” species. The high degree of morphological diversity among these infraorders has led to a dynamic classification and conflicting hypotheses of evolutionary relationships. In this study, we estimated phylogenetic relationships among the major groups of all lobster families and 94% of the genera using six genes (mitochondrial and nuclear) and 195 morphological characters across 173 species of lobsters for the most comprehensive sampling to date. Lobsters were recovered as a non-monophyletic assemblage in the combined (molecular + morphology) analysis. All families were monophyletic, with the exception of Cambaridae, and 7 of 79 genera were recovered as poly- or paraphyletic. A rich fossil history coupled with dense taxon coverage allowed us to estimate and compare divergence times and origins of major lineages using two drastically different approaches. Age priors were constructed and/or included based on fossil age information or fossil discovery, age, and extant species count data. Results from the two approaches were largely congruent across deep to shallow taxonomic divergences across major lineages. The origin of the first lobster-like decapod (Polychelida) was estimated in the Devonian (~409–372 Ma) with all infraorders present in the Carboniferous (~353–318 Ma). Fossil calibration subsampling studies examined the influence of sampling density (number of fossils) and placement (deep, middle, and shallow) on divergence time estimates. Results from our study suggest including at least 1 fossil per 10 operational taxonomic units (OTUs) in divergence dating analyses. [Dating; decapods; divergence; lobsters; molecular; morphology; phylogenetics.]

Lobsters (Achelata, Astacidea, Glypheidea, Polychelida) are a morphologically diverse and economically important assemblage of decapod crustaceans with a rich fossil record dating back ~360 Ma (Schram and Dixon 2004). These include the clawed, slipper, furry, coral, spiny, and deep-sea blind lobsters, crayfish and “living fossil” glypheids (Fig. 1). Although lobsters all have a superficially similar body plan, the morphological and ecological diversity is astonishing. Species range from clawed to clawless, sighted to blind, and ornamented to undecorated body forms inhabiting deep to shallow, cave to surface, and freshwater to marine ecosystems. A rich fossil record allows us to

estimate the origins and diversification of major lineages while exploring the emergence of morphological and ecological diversity.

Apart from their diversity, many types of lobsters have significant economic, conservation, and cultural values. Commercial fisheries and aquacultures rely on representatives within Achelata and Astacidea to bring in billions of dollars each year to an international economy for both human consumption and the aquarium trade (Steneck et al. 2011). Overexploitation of marine resources has led to increased conservation and management efforts on commercially important species, whereas others may be vulnerable due to

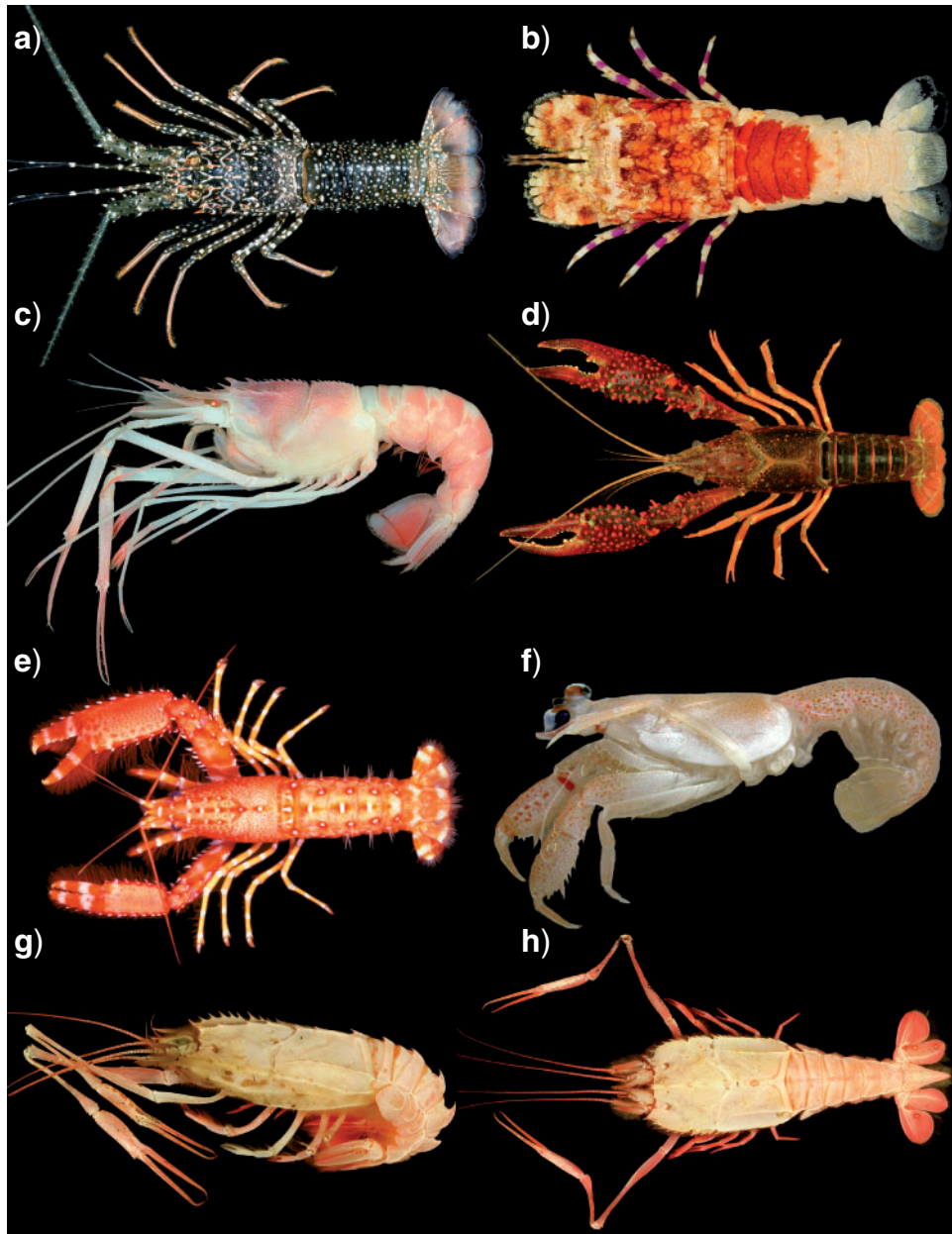


FIGURE 1. Lobster-like decapod representatives; Achelata: A, *Panulirus guttatus* ULLZ 3497; B, *Scyllarus chacei* ULLZ 6596; Astacidea: C, *Acanthacaris caeca* ULLZ 7574; D, *Procambarus clarkii* ULLZ 11947; E, *Enoplometopus antillensis* ULLZ 3623; Glypheidea: F, *Laurentaeglyphea neocaledonica* MNHN:IU200814773; Polychelida: G, H, *Stereomastis sculpta* ULLZ 8022 (Photo credits: A-E, F-H: DL Felder, F: Richer de Forges, 2006).

rarity in nature (e.g., Glypheidea). Lobsters are not only economically important, but also contribute to the cultural livelihood of many communities that celebrate these delicacies through festivals, crayfish boils, and other social activities (Swahn 2004; Jones et al. 2006).

Resolving the phylogenetic relationships among and within lobster-like decapods will aid in fishery and conservation efforts, biodiversity estimates, and an increased evolutionary understanding; however, current phylogenetic hypotheses are dynamic and under continuous debate (Fig. 2) (Scholtz and Richter 1995; Dixon et al. 2003; Ah Yong and Meally 2004; Tsang et al.

2008; Bracken et al. 2009; Toon et al. 2009; Karasawa et al. 2013). Recent molecular studies using nuclear protein coding genes recovered lobster-like decapods as a monophyletic group with high support, whereas alternative studies using both molecules and/or morphology found otherwise. Although these studies are progressive in the understanding of lobster-like evolution, many lack significant taxon representation and/or combined evidence (molecules + morphology).

Lobsters have a rich fossil record due to the enhanced preservation of their exoskeleton. Interestingly, current species' richness does not adequately reflect the fossil

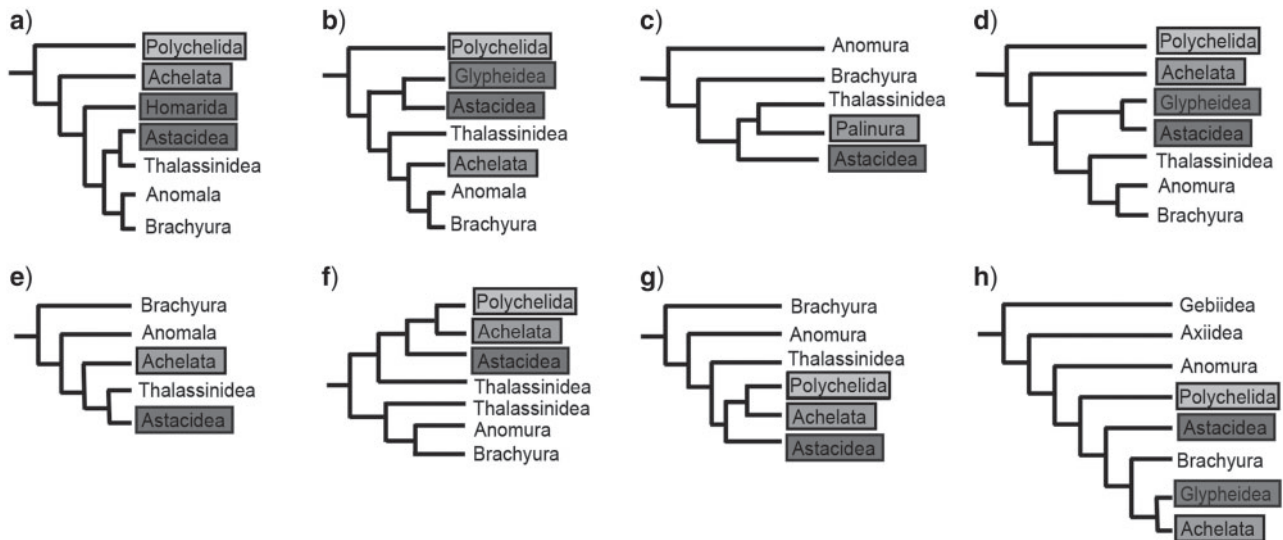


FIGURE 2. Hypotheses of higher level lobster relationships based on morphological cladistic analyses (a, b) and molecular phylogenetic analyses (c–h). (a) Scholtz and Richter (1995); (b) Dixon et al. (2003); (c) Crandall et al. (2000); (d) Ahyong and O’Meally (2004); (e) Porter et al. (2005); (f) Tsang et al. (2008); (g) Toon et al. (2009); (h) Bracken et al. (2009).

history of lobster-like decapods and until recently, some major lineages were only known as fossil species. The infraorder Glypheidea was thought to be extinct until 1975, when *Neoglyphea inopinata* was described from the Philippines (Forest and de Saint Laurent 1975, 1976). Today, the glypheids are considered “living fossils,” with only two extant species that very closely resemble their extinct relatives. Their fossil record is the most numerous with over 256 fossil species discovered, with their highest diversity during the Jurassic (~147 species, Schweitzer et al. 2010). Astacidea, with over 653 extant taxa contains ~124 fossil species, whereas Polychelida and Achelata contain 38 and 140 extant and 55 and 72 extinct species, respectively. The integration of fossil and/or geological data with molecular and morphological data adds directionality to the major events and transitions that occurred during the evolution of a group.

Divergence time analyses are commonly implemented in modern-day evolutionary studies, and some have evaluated the performance and error associated with the various dating methods (Perez-Losada et al. 2004; Rutschmann et al. 2007; Battistuzzi et al. 2010; Inoue et al. 2010; Lukoschek et al. 2012). Our study is unique due to the large number of fossil priors (28 calibrations) and taxa (195 individuals) included, allowing us to examine how sampling density (number of fossils) and fossil placement (deep, middle, and shallow) influence divergence time estimates across our phylogeny. Here, we subsample our 28-fossil data set (“inclusive” data set) and based on five performance criteria we assess the performance of each subsampled data set (i.e., 1, 4, 8, 12, 16, 20, and 24 fossils). In addition to subsampling, and for the first time, we compare divergence time estimates using drastically different construction of age priors. Priors were constructed and/or included based on: (i) fossil age information (referred herein as “28 fossil” analysis) or (ii) fossil discovery, age,

and extant species counts, a novel Bayesian Posterior Branching Process (referred herein as “BPBP”) approach (Wilkinson et al. 2011). The method proposed by Wilkinson et al. (2011) estimates fossil calibration dates using a model of speciation and fossil recovery (Wilkinson and Tavaré 2009). The number of fossils discovered throughout history and their geological age distribution, in combination with extant species counts, are then used to update these prior distributions to give posterior distributions for the node ages given the information in the entire fossil record. Both approaches were implemented using Bayesian evolutionary analysis by sampling trees (BEAST) in order to assess congruence of current methods.

Here, we present the most comprehensive sampling of lobster-like decapods (94% of all extant genera), combining nuclear and mitochondrial sequences with morphological characters, to generate the largest phylogeny of the group to date. We examine the evolutionary relationships among infraorders, families, genera, and species and compare our findings with current hypotheses and taxonomic classifications. A rich fossil record allows us to estimate the divergence times and origins of major lineages. By implementing different dating approaches (28 fossil and BPBP), we can compare congruence across methods. In addition, we subsample the fossil data set to examine the influence of calibration density on divergence time estimation.

MATERIALS AND METHODS

Taxon Sampling

A total of 173 species (201 specimens) of lobster-like decapods (Astacidea, Achelata, Polychelida, Glypheidea) were included in the analysis (Supplementary

Appendix S1, <http://dx.doi.org/10.5061/dryad.4v875>). Only three genera from Astacidea (*Homarinus*, *Thymopsis*, and *Distocambarus*) and two from Polychelida (*Cardus* and *Homeryon*) were not included owing to unavailability of molecular-grade tissues. Classification of these infraorders follows the molecular and morphological studies that find Palinura to be polyphyletic (Scholtz and Richter 1995; Dixon et al. 2003; Ah Yong and Meally 2004) and recognize the polychelids and glypheids as separate lineages (Tsang et al. 2008; Ah Yong 2009; Bracken et al. 2009; Boisselier-Dubayle et al. 2010). To recover generic-level relationships, we attempted to sample at least three species per genus, with denser sampling within taxonomically diverse and problematic groups. New sequences are deposited in GenBank, whereas others were obtained directly from GenBank (Supplementary Appendix S1, <http://dx.doi.org/10.5061/dryad.4v875>). As the overall monophyly of the lobsters is contentious, 3–5 species from major decapod lineages (Dendrobranchiata, Caridea, Brachyura, Anomura, Axiidea, Gebiidea) were selected as outgroups. All outgroup sequences were obtained from GenBank (Supplementary Appendix S1, <http://dx.doi.org/10.5061/dryad.4v875>).

Gene Selection

As the lobsters represent diverse and ancient groups with the earliest lineages originating ~340–360 Ma (Schram et al. 1978; Schram and Dixon 2004; Bracken et al. 2010), we chose markers useful in resolving relationships at both deep and shallow taxonomic levels across broad time scales. In recent years, the Decapod Tree of Life project has established a set of genetic markers proven to be informative at fine and coarse evolutionary scales (Bracken et al. 2009; Felder and Robles 2009; Robles et al. 2009; Toon et al. 2009). From these markers, we selected three mitochondrial (16S, 12S, COI) and three nuclear genes (18S, 28S, H3) for inclusion in the molecular analysis. The same gene set was also used in the combined data set (molecular + morphological).

Morphological Data

The morphological data matrix was constructed in MacClade 4.0 and consisted of 190 characters and 229 terminals (Supplementary Appendices S2 and S3; <http://dx.doi.org/10.5061/dryad.4v875>). Characters for external morphology (characters 1–183, 189, 190) were scored individually for each species sequenced for analysis. Codings were derived from published accounts and specimens in the collections of the Australian Museum; National Museum of Natural History, Raffles Museum of Biodiversity Research, National University of Singapore; National Museum of Natural History, Smithsonian Institution; Muséum national d'Histoire, Paris; National Taiwan Ocean University; and Queensland Museum. For histological and developmental characters (characters 184–188) that are highly conserved across infraorders, reasonable assumptions of monophyly were made. Thus, for these

conserved characters, all members of a particular infraorder for which data were available for some members were scored as uniform. For example, a high number of ectoteloblasts in embryonic growth zone (40 versus 19), uniquely apomorphic for the freshwater crayfish, is scored as uniform for that group, even though it has not been assayed for every genus and species analyzed herein. Missing data were scored as unknown (?) and polymorphisms were scored as such rather than assuming a plesiomorphic state. Inapplicable character states were scored as unknown (but indicated as “-”) rather than as a fifth character state “inapplicable” to avoid the possibility of nodes being supported by a non-existent character state.

DNA Extraction, Polymerase Chain Reaction, and Sequencing

Genomic DNA was extracted from the gills, abdomen, pereopod or pleopod using the Qiagen DNeasy® Blood and Tissue Kit (Cat. No. 69582), QIAamp DNA Mini Kit (Cat. No. 51304) or QIAamp DNA Micro Kit (Cat. No. 56304). Gene regions were amplified with the polymerase chain reaction (PCR) using one or more sets of primers. Regions of the following genes were sequenced: 16S large ribosomal subunit (~550 bp, Crandall and Fitzpatrick 1996), 12S small ribosomal subunit (~400 bp, Buhay et al. 2007), cytochrome oxidase 1 (COI) protein coding gene (~650 bp, Folmer et al. 1994), 28S large ribosomal subunit (~2500 bp, Whiting et al. 1997; Whiting 2002; Palero et al. 2008), 18S small ribosomal subunit (~1800 bp, Medlin et al. 1988; Whiting et al. 1997; Apakupakul et al. 1999; Whiting 2002; Bracken et al. 2009), and protein-coding histone 3 (H3) (~350 bp, Colgan et al. 1998).

PCR amplifications were performed in 25–50 µL volumes containing 1 U of Taq polymerase (HotMaster, AccuPrime or REDTaq), PCR Buffer, 2.5 mM of deoxyribonucleotide triphosphate mix (dNTPs), 0.5 µM forward and reverse primer, and 30–100 ng extracted DNA. The thermal profile used an initial denaturation for 1 min at 94 °C followed by 30–40 cycles of 30 s to 1 min at 94 °C, 45 s to 1 min at 46–58 °C (depending on gene region), 1 min at 72 °C and a final extension of 7 min at 72 °C. PCR products were purified using filters (PrepEase™ PCR Purification 96-well Plate Kit, USB Corporation) and sequenced with ABI BigDye® terminator mix (Applied Biosystems, Foster City, CA). Cycle Sequencing reactions were performed in an Applied Biosystems 9800 Fast Thermal Cycler (Applied Biosystems), and sequencing products were run (forward and reverse) on an ABI 3730×1 DNA Analyzer 96-capillary automated sequencer in the Brigham Young University (BYU) sequencing center.

Phylogenetic Analyses

Sequences were cleaned, edited, and assembled using Sequencher 4.8 (GeneCodes, Ann Arbor, MI, USA). To

check for pseudogenes, we followed suggestions by Song et al. (2008) by extracting DNA from tissue with high amounts of mitochondria (gill tissue), translating protein-coding sequences (COI, H3) to check for indels and stop codons, comparing sequences to closely related species and building individual gene trees to ensure similar topologies. Individual gene alignments were performed in MAFFT. As our data set contained multiple genes with conserved domains and large gaps (16S, 12S, 18S, and 28S), we used the “E-INS-i” option in MAFFT. For non-coding genes, GBlocks v0.91b was used to exclude regions of questionable positional homology (Castresana 2000; Talavera and Castresana 2007). Individual gene data sets were concatenated in MESQUITE 2.73 (Maddison and Maddison 2010) and partitioned in the final analyses. To help select the optimal partitioning strategy for our data set, Partition Finder (Lanfear et al. 2012) was implemented using AIC criteria. We explored both a 10-partition scheme (by gene and codon) and 6-partition scheme (by gene). In addition to PartitionFinder, we used the Bayesian Information Criterion (BIC) (Schwarz 1978) in MODELTEST to determine the best model of evolution for each individual molecular data set (Posada and Crandall 1998).

Before concatenation individual gene/morphology trees were generated using randomized accelerated maximum likelihood (RAxML) (Stamatakis et al. 2005, 2007, 2008) and maximum parsimony methods to identify conflicting histories and identify contamination taxa (see below for detailed methods, Supplementary Appendices S4–S8; <http://dx.doi.org/10.5061/dryad.4v875>). Individual gene sets were concatenated and two final data sets were generated (i) molecular and (ii) molecular + morphology (combined). The same gene set was used in both analyses. To explore congruence between concatenation and species tree methods, the program, iGTP (Chaudhary et al. 2010) was used to infer a species tree phylogeny from gene trees (Supplementary Appendix S9, <http://dx.doi.org/10.5061/dryad.4v875>). In iGTP four gene trees (mitochondrial, H3, 28S, and 18S) were used to estimate a species tree using the minimize deep coalescence model with the leaf-adding algorithm for 1000 hill-climbing heuristic searches.

The maximum likelihood (ML) analysis was conducted on the molecular data set(s) using RAxML (Stamatakis et al. 2005, 2007, 2008). We used a total of 400 searches for the best ML tree (200 from random, 200 from bootstrap starting trees). ML estimates were compared to determine the best tree and bootstraps were mapped on the resulting topology. Likelihood settings followed the General Time Reversible model (GTR) with a γ -distribution. RAxML estimated all free parameters following a partitioned data set. Confidence in the resulting topology was assessed using non-parametric bootstrap estimates (Felsenstein 1985) with 1000 pseudoreplicates and values >60% are presented on the resulting phylogeny (Supplementary Appendix S10, <http://dx.doi.org/10.5061/dryad.4v875>). In addition

to implementing a GTRGAMMA model in RAxML, we also explored the use of a site-heterogeneous CAT-based model in Phylobayes (Lartillot and Philippe 2004; Lartillot et al. 2009). Although CAT-based models have been used less frequently in nucleotide data sets when compared with amino acids, they have shown to be more effective at dealing with site heterogeneity in phylogenomic studies examining deep-level divergences. In Phylobayes, constant sites were removed from the alignment and two independent Markov chains were run with a total length of 25 220 cycles. After burn-in, a consensus tree was recovered with posterior probabilities noted on resulting phylogram (Supplementary Appendix S11, <http://dx.doi.org/10.5061/dryad.4v875>).

The Bayesian (BAY) analysis was conducted in MrBayes v3.1.2b4 (Huelsenbeck and Ronquist 2001) for the molecular data set and combined data set (molecular + morphological). For the morphological characters, we used the Markov k (Mk, Lewis 2001) model with equal state frequencies, combined with γ -distributed rates across sites. We implemented a “coding = variable” parameter to use the likelihood conditional on character variability, rather than the ordinary likelihood, which assumes that there will be an appropriate number of constant characters present. Three independent runs were performed (each consisting of 20 chains and nswaps =10) on each data set (molecular and combined). Each analysis ran for 50 000 000 iterations, which we thinned to every 1000th iteration. Trace plots were visually inspected to assess convergence, mixing, and stationarity in Tracer v1.4. (Rambaut and Drummond 2007). Once the split frequency in each analysis was 1% (reached after around 8 and 3 million generations for the molecular and combined analysis, respectively), a 50% majority-rule consensus tree was obtained from the remaining saved trees. Posterior probabilities (PPs) for clades were compared for congruence and then combined between individual analyses. Values >0.7 are presented on the BAY phylograms (Fig. 3a,b; Supplementary Appendix S10, <http://dx.doi.org/10.5061/dryad.4v875>). All ML and BAY analyses were performed on the Marylou5 Dell PowerEdge M610 computing cluster at Brigham Young University and/or the High Performance Computing Cluster (Panther) at Florida International University.

Divergence Time Analyses

We used two approaches to estimate the relative timing of divergence between lobster lineages. Both methods used a relaxed molecular clock model, which allows the rate of evolution to vary among lineages. Fossil observations were used to calibrate the molecular clock, thus separating rate and time and allowing the estimation of divergence times. An MCMC algorithm was used to sample from the joint posterior distribution of divergence times, branch rates, and substitution

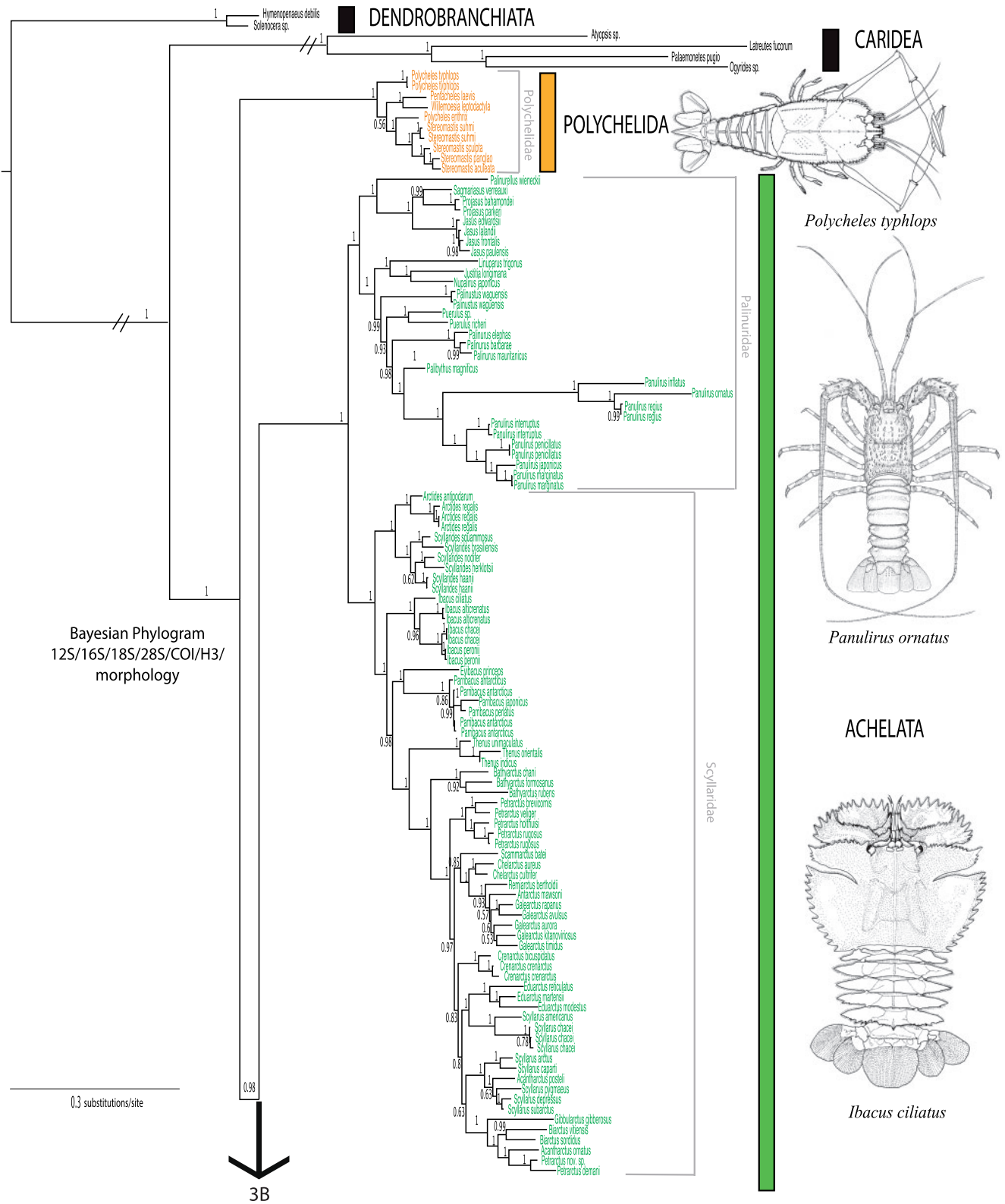
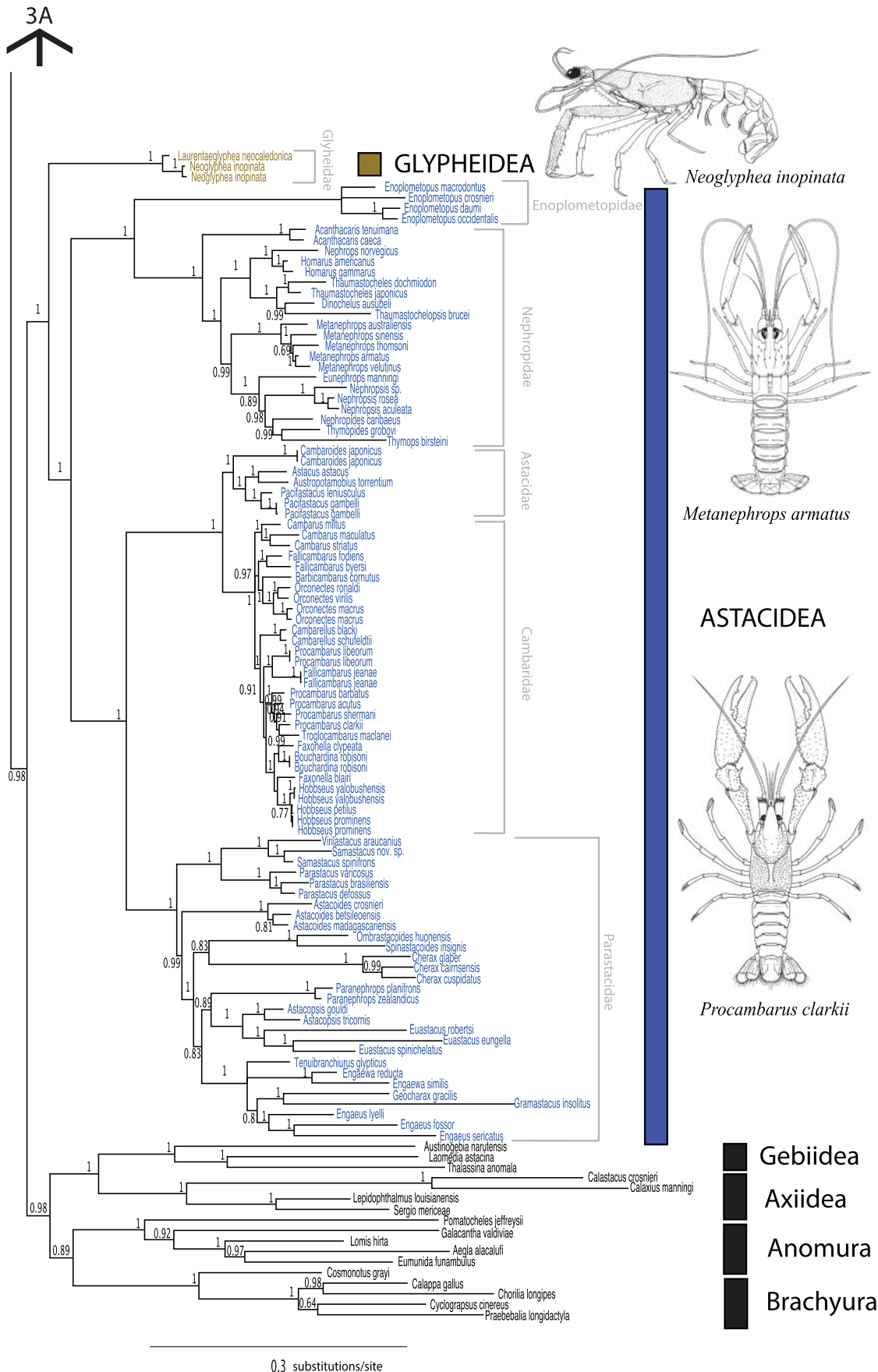


FIGURE 3. (a, b) Combined Bayesian phylogram based on molecular (4982 characters) and morphological (190 characters) data. Thick vertical bars represent lobster-like infraorders or other decapod lineages (infraorders, suborders). Bayesian posterior probabilities $P > 0.56$ are noted above or below branches.



Downloaded from <http://sysbio.oxfordjournals.org/> at University of Nottingham on July 29, 2014

FIGURE 3. Continued

model parameters. The primary difference between the methods lies in the prior distributions used to reflect uncertainty in the divergence time calibrations (see Methods 1 and 2 below).

Drummond et al. (2006) propose an uncorrelated relaxed clock, which relaxes the assumption of autocorrelation and allows the rate at each branch to be drawn independently from an underlying rate distribution. Calibration uncertainty can be described using one of several available parametric distributions implemented in the BEAST software package (Drummond and Rambaut 2007). For the first dating method we used a common approach, where all priors were based on fossil age information (Method 1 = 28-fossil age model). The second method, proposed by Wilkinson et al. (2011), differs in the way paleontological data are incorporated. Rather than using user-specified priors based on the age of the fossil, fossil calibration dates are estimated from the fossil record, using a model of speciation, fossilization, and recovery to formulate prior distributions for node ages (Wilkinson and Tavaré 2009). The number of fossils discovered throughout history and their geological age distribution, in combination with extant species counts, are then used to update these prior distributions to give posterior distributions for the node ages, given the information in the entire fossil record. The benefit of using this BPBP model is that it moves the subjective judgments further from important quantities and enables the utilization of more of the fossil record, thus letting data play a larger role in the analysis. These posterior distributions are then used as prior distributions in the molecular analysis implemented in BEAST (Method 2 = BPBP model).

Fossils, Time Calibrations, and Prior Construction

Method 1: 28-fossil age model.—We included a total of 28 calibration points that represent lineages at both deep, middle, and shallow nodes within our divergence time analysis (Table 1; Fig. 4; Supplementary Appendix S12; <http://dx.doi.org/10.5061/dryad.4v875>). We followed recommendations by Parham et al. (2012) when justifying fossil placement and selection and consulted with decapod paleontologists (co-authors Feldmann and Schweitzer) to help with assignments. When possible, each fossil used for calibration was based on a single specimen that could be unambiguously assigned to a clade. In some cases the fossils were assigned based on fragmentary specimens or direct observation of conspecifics; nevertheless, diagnostic characteristics (i.e., chela, pleonites, uropods) for each assignment were identified (Supplementary Appendix S12; <http://dx.doi.org/10.5061/dryad.4v875>). In addition, an apomorphy-based diagnosis of each fossil was performed and any fossil that showed inconsistency with our combined total evidence topology is discussed (Supplementary Appendix S12; <http://dx.doi.org/10.5061/dryad.4v875>). Ages were assigned based on original publications for the fossil. In

all cases, Feldmann and Schweitzer either described the fossil specimen, directly observed individuals and/or thoroughly reviewed the literature to justify inclusion of the fossil in the study (Schweitzer et al. 2010; Table 1). For all fossil calibrations, we chose the oldest known fossil representative and assigned this age to either the crown (MRCA, most recent common ancestor) or stem node (i.e., node preceding the crown node) based on the above mentioned apomorphy diagnosis (Parham et al. 2012). In BEAST, an exponential prior was implemented on all fossil calibrations, with the offset values set to the minimum calibration age. This distribution is suitable for modeling fossil calibrations, because the probability decreases with a growing discrepancy between estimated nodal age and the age of the calibrating fossil (Ho 2007). The choice of an exponential prior allows us to ascribe the greatest probability within the age range associated with fossil discovery, while avoiding a hard minimum age.

Method 2: BPBP model.—Unlike the previous approach, the fossil calibration dates are estimated rather than specified. The number of fossilized species (count data) found during each epoch was recorded for each of the major lineages (Astacidea, Achelata, Polychelida, Glypheidea) (Table 2). If a fossil species was found more than once in different epochs, it was recorded for each epoch in which it was found. If one specimen of a single species spanned multiple time intervals (epochs) (i.e., the time and error intervals associated with its discovery overlapped multiple epochs), that specimen was accounted for randomly in one of the multiple epochs that it spread. A random assignment of the specimen allowed us to avoid biasing its placement in the table. Extant species counts were taken from De Grave et al. (2009). Time intervals of epochs and ages followed the 2009 Geological Time Scale provided by the Geological Society of America (Walker and Geissman 2009).

As interest lies in the lobster-like decapods divergence dates, we assumed an evolutionary tree (Polychelida, [Achelata, {Astacidea, Glypheidea}]). We assigned τ_1 to be the date the (Achelata, Astacidea, Glypheidea) split from the Polychelida, τ_2 to be the date Achelata split from the (Astacidea, Glypheidea), and τ_3 to be the date the Astacidea split from the Glypheidea. The two oldest lobster-like fossils (Mississippian, Late Devonian; Table 2) were included as stem fossils in the analysis, because they share morphological characteristics that allied them to other lobster-like decapods, but we could not confidently assign them to a single infraorder. We used a uniform prior distribution for τ_1 , setting the minimum bound using the oldest fossil representative (*Palaeopalaemon newberryi*, Late Devonian—Table 2), and used an arbitrary large maximum bound of 685 Ma (i.e., $\tau_1 \sim U[-685, -385]$ a priori). The posterior distribution was found to be robust to the choice of maximum bound (as long as a large value is used). To complete the prior specification, we specified an ordering of node

TABLE 1. Fossil calibrations used in divergence time analyses (28-fossil run, BEAST)

Taxonomy	Species	Geological age (Ma)	Node
Outgroup			
Natantia			
Suborder Dendrobranchiata			
Superfamily Penaeoidea	<i>Aciculopoda mapesi</i> (Feldmann and Schweitzer 2010)	Fammenian (Devonian), 354–364	1
Suborder Pleocyemata			
Infraorder Caridea	<i>Pinnacaris dentata</i> (Garassino and Teruzzi 1993)	Late Triassic, Norian, 210–221	2
Reptantia			
Infraorder Axiidea	<i>Palaeopalaemon newberryi</i> (Whitfield 1880)	Late Devonian, 354–370	3
Infraorder Gebiidea	<i>Callianassa</i> s.l. <i>bonjourii</i> (Etallon 1861)	Early Jurassic, Toarcian, 180–190	12
Infraorder Anomura	<i>Upogebia obscura</i> (Von Meyer 1834)	Early Triassic, 242–248	11
	<i>Platykotta akaina</i> (Chablais, Feldmann and Schweitzer 2010)	Late Triassic, Norian/Rhaetian, 206–221MYA	7
Ingroup			
Infraorder Glypheidea			
Family Glypheidae	<i>Litogaster turnbullensis</i> (Schram 1971)	Early Triassic, 242–248	5
Infraorder Astacidea			
Superfamily Enoplometoidea	<i>Uncina ollerenshawii</i> (Feldmann and Copeland 1988) and <i>Uncina pacifica</i> (Schweigert et al. 2003)	Early Jurassic, Pliensbachian, 180–206	10
Superfamily Nephropoidea	<i>Pseudastacus pusillus</i> (Van Straelen 1924 [imprint 1925])	Middle Jurassic, Bajocian, 169–176	6
Genus <i>Homarus</i>	<i>Homarus travisensis</i> (Stenzel 1945)	Early Cretaceous, Albian, 99–112	21
Genus <i>Metanephrops</i>	<i>Metanephrops rossensis</i> (?)	Late Cretaceous, Campanian, 71.3–83.5	22
Family Astacidae	<i>Palaeocambarus licenti</i> (Van Straelen 1928c)	Early Cretaceous, 99–144	13
Genus <i>Austropotamobius</i>	<i>Austropotamobius llopisi</i> Via 1971	Late Jurassic, Kimmeridgian, 151–154	23
Genus <i>Astacus</i>	<i>Astacus multicaovatus</i> (Bell 1863)	Early Cretaceous, Berriasian-Hauterivian, 127–144	24
Genus <i>Pacifastacus</i>	<i>Pacifastacus chenoderma</i> (Cope 1871)	Miocene, 5.3–23.8	25
Family Parastacidae	<i>Palaeoecchinastacus australianus</i> (Martin et al. 2008)	Early Cretaceous, 99–144	8
Genus <i>Astacopsis</i>	<i>Astacopsis franklini</i> (Gray 1845)	Pleistocene, 0.01–1.8	27
Genus <i>Paranephrops</i>	<i>Paranephrops fordycei</i> (Feldmann and Pole 1994)	Miocene, 5.3–23.8	28
Genus <i>Procambarus</i>	<i>Procambarus primaevus</i> (Packard 1880)	Early Cenozoic, 65?	26
Infraorder Achelata			
	<i>Yunnanopalinura schrami</i> (Feldmann et al. 2012)	Middle Triassic, Anisian 241–247	4
Genus <i>Biarctus</i>	<i>Biarctus vitiensis</i> (Dana et al. 1852a)	Pleistocene, 0.01–1.8	20
Genus <i>Parribacus</i>	<i>Parribacus cristatus</i> (Forster 1984)	Eocene, 33.7–54.8	18
Genus <i>Scyllarides</i>	<i>Scyllarides bolcensis</i> (De Angeli and Garassino 2008)	Eocene, 33.7–54.8	16
Genus <i>Scyllarus</i>	<i>Scyllarus junghumi</i> (Bohm 1922)	Miocene, 5.3–23.8	19
Family Palinuridae	<i>Archaeopalinurus</i> (Pinna 1974)	Late Triassic, Norian, 210–221	9
Genus <i>Jasus</i>	<i>Jasus flemingi</i> (Glaessner 1960)	Miocene, 5.3–23.8	17
Genus <i>Justitia</i>	<i>Justitia vicetina</i> (Beschinn et al. 2001)	Eocene, 33.7–54.8	15
Genus <i>Linuparus</i>	<i>Linuparus carteri</i> (Reed 1911)	Early Cretaceous, Aptian, 112–121	14

Note: Number corresponds to nodal placement as assigned in Figures 4.

ages, $\tau_1 > \tau_2 > \tau_3$, and gave a hard minimum age for the other two divergence dates: $\tau_2, \tau_3 < -260$ Ma. This tree was assumed based on the phylogenetic analysis (Fig. 3a,b).

A logistic model of expected diversification was used, which is equivalent to assuming diversification commences rapidly and then slows or remains constant thereafter (see Equation (3) in Wilkinson et al. 2011). The three parameters in this equation were given the following priors: $\rho \sim U [0.01, 0.4]$ so that diversity was expected to reach 90% of the final expected diversity between 10 and 800 Ma after time of origin; parameter

$\gamma \sim U [0.001, 0.02]$ so that the expected modern diversity ranged between 100 and 2000 species; for λ we specified $1/\lambda \sim U [1, 20]$, so that the expected period of time for each species existed was between 1 and 20 Ma. Fossil preservation and discovery was modeled using a Poisson process model, with constant discovery rate per unit of time. The posterior mean fossil discovery rate was estimated to be 0.01, which equates to an average of one fossil find, per species, per 100 Ma. To fit the model to the fossil data in Table 2, we used an ABC rejection algorithm, using the metric given by Equation (5) in Wilkinson et al. (2011), with the same tolerance at

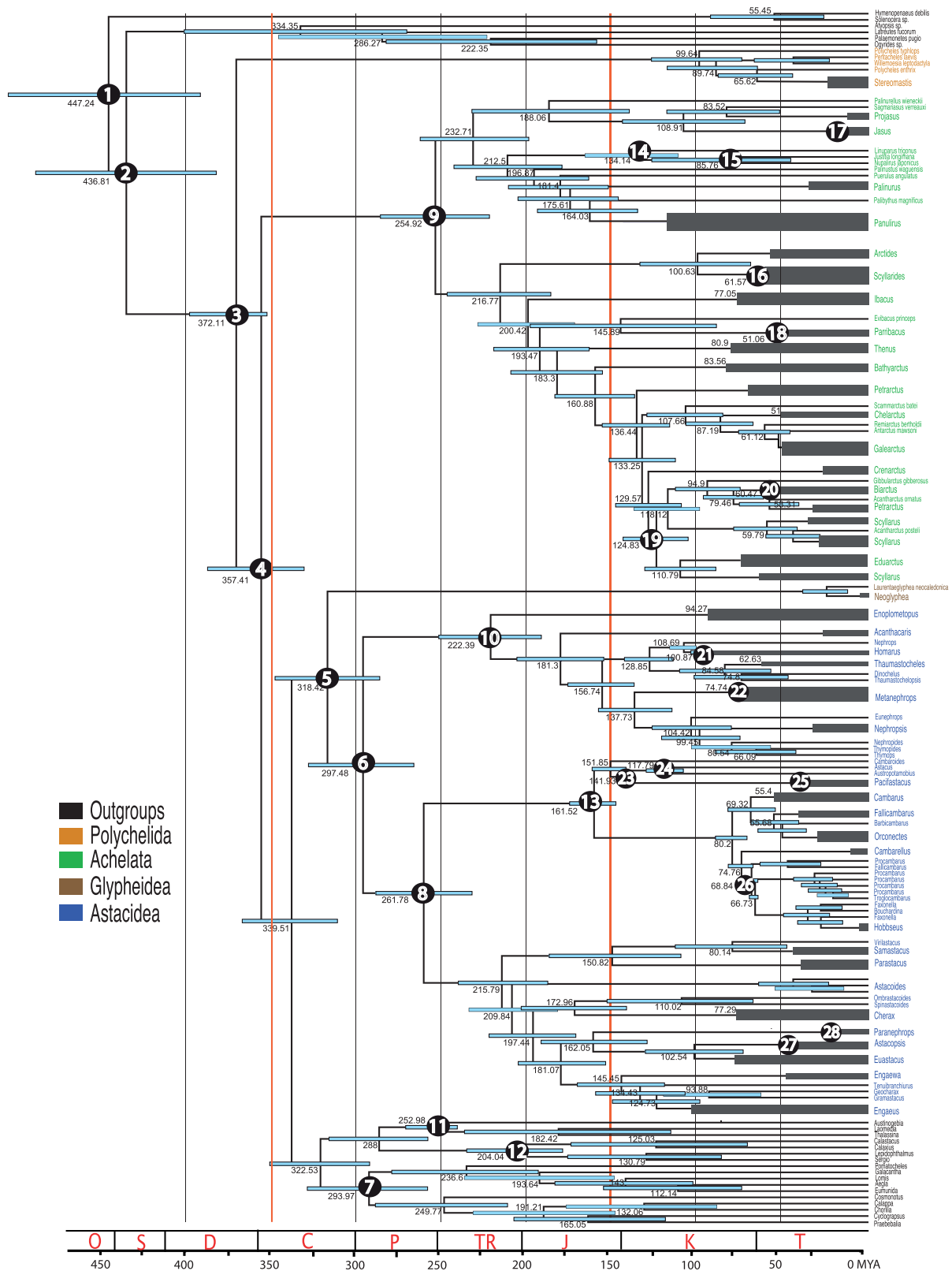


FIGURE 4. Divergence time chronogram using 28-fossil approach in BEAST. Fossil calibration points are indicated by numbers 1–28 embedded in black circles. Divergence time estimates (Ma) are noted adjacent to their respective nodes and blue nodal bars correspond to the 95% highest posterior density regions. Red vertical line divides the chronogram into three regions for fossil calibration placement; deep, middle, and shallow. Geological periods are superimposed onto the phylogeny and listed as follows: O, Ordovician; S, Silurian; D, Devonian; C, Carboniferous; P, Permian; TR, Triassic; J, Jurassic; K, Cretaceous; T, Tertiary. Colored taxa correspond to the lobster-like decapod infraorders. Orange = Polychelida, Green = Achelata, Brown = Glypheidea, Blue = Astacidea.

TABLE 2. A summary of fossil count data used in the BPPB model

Epoch	k	Time at base of interval k (Ma)	Fossil counts: Poly+ Ach+ Gly+Ast	Fossil counts: Ach + Gly + Ast	Fossil counts: Gly + Ast
Extant	0	0.0	833	795	655
Pleistocene	1	-2.6	5	5	4
Pliocene	2	-5.3	4	4	4
Miocene	3	-23.0	10	10	6
Oligocene	4	-33.9	7	6	4
Eocene	5	-55.8	32	32	20
Paleocene	6	-65.6	15	15	10
Late Cretaceous	7	-99.6	140	137	106
Early Cretaceous	8	-145.5	86	85	76
Late Jurassic	9	-161.0	95	83	78
Middle Jurassic	10	-176.0	43	37	37
Early Jurassic	11	-201.6	70	48	47
Late Triassic	12	-235.0	18	12	11
Middle Triassic	13	-245.0	16	16	16
Early Triassic	14	-251.0	5	5	5
Late Permian	15	-260.0	2	2	2
Middle Permian	16	-271.0	0	0	0
Early Permian	17	-299.0	0	0	0
Pennsylvanian	18	-318.0	0	0	0
Mississippian	19	-359.0	1	0	0
Late Devonian	20	-385.0	1	0	0
Pre-mid-Devonian	21	/	0	0	0

Note: The table is divided into epochs with the time for each epoch given in millions of years (Ma).

Poly, Polychelida; Ach, Achelata; Ast, Astacidea; Gly, Glypheidea.

all three nodes: $\varepsilon_1 = \varepsilon_2 = \varepsilon_3 = 0.45$. For more details, see Wilkinson et al. (2011).

Analytic approximations for the posterior.—After experimenting with a range of distributions, we found that fitting independent skew- t distributions (Azzalini and Genton 2007) to each posterior gave the most acceptable parametric fit. The skew- t distribution is parameterized by four parameters: location, scale, shape, and the number of degrees of freedom. As we could not implement a skew- t distribution in BEAST, we fit each posterior to a lognormal (τ_2 , τ_3) or exponential distribution (τ_1) (Supplementary Appendix S13; <http://dx.doi.org/10.5061/dryad.4v875>). A recent study has shown this distribution choice in BEAST produces similar posterior estimates and 95% highest posterior density regions (HPDs) when compared with using the skew- t distribution in mcmctree (Warnock et al. 2012). The lognormal distribution is parameterized by the mean, offset, standard deviation and the exponential distribution is parameterized by the mean and offset, all shown in Supplementary Appendix S13 (<http://dx.doi.org/10.5061/dryad.4v875>).

Bayesian Evolutionary Analysis by Sampling Trees

The data set was partitioned by gene and assigned independent models of evolution as in previous analyses. Branch rates are assumed to be independently

drawn from a log normal distribution, and a Yule prior (constant lineage birth rate) is used to describe the rate of speciation. We recognize that there is a variety of models to consider when using relaxed dating methods. Studies that have compared uncorrelated and autocorrelated rates have recovered conflicting results, with some favoring uncorrelated models (Drummond et al. 2006), others favoring autocorrelated models (Lepage et al. 2007) and some favoring both (autocorrelated and uncorrelated) depending on the data set (Ronquist et al. 2012). We settled on using an uncorrelated model due to the taxonomic level of interest (focused at infraorder, family and genus level), age of the group (oldest fossil ~ 360 Ma), and evidence based on divergence time analysis, which measures rate autocorrelation on neighboring branches (Ho 2009; Drummond et al. 2006). In order to compare results, we used a starting tree (combined Bayesian consensus tree, see phylogenetic analysis, Fig. 3a,b) and removed the tree searching parameter from our BEAUTI xml file. As we need to provide a starting tree that satisfies the topological and temporal constraints associated with integrating fossil calibrations, we made the branch lengths proportional to timing (chronogram) rather than substitutions per site (phylogram), using the non-parametric rate smoothing algorithm in r8s (Sanderson 2003). We ran two independent runs for 350 000 000 iterations, which we thinned to every 10 000th iteration. Trace plots were visually inspected to assess convergence, mixing, and stationarity in Tracer v1.4. Convergence diagnostics were calculated using the CODA package in R (Plummer et al. 2006); the last 20 000 samples from each chain were used for further analysis with the previous samples discarded. Estimates of the mean divergence times with 95% HPD and posterior probabilities (represented as percentages) are noted on the chronogram (Fig. 4). All BEAST analyses were performed on the Marylou6 Dell PowerEdge M610 computing cluster at Brigham Young University or the High Performance Panther Cluster at Florida International University. For all analyses we examined the affect of priors on the posterior distributions when the data set is run without the data (empty alignment generated from BEAUTI).

Fossil Calibration Subsampling

We examined the range of calibrations used in previous analyses by searching the Web of Science using the keywords to “divergence dating,” refined by “fossil.” We narrowed the search to literature published after 2005 to capture studies using the methods herein (i.e., BEAST). We examined across 165 references for (i) number of fossils and (ii) number of terminals included, and (iii) divergence method used. Our literature search revealed that the 28 fossils used in this analysis represent one of the most fossil-rich data sets to date. This data set provides a unique opportunity to test the sensitivity of divergence time estimation to fossil calibration priors. In particular, we were interested in the effect of sampling

density (number of fossil calibrations) on node age estimates. More specifically, at what point does the addition of fossil calibrations only slightly affect age estimation across a phylogeny? In this analysis, we randomly subsampled from within the set of 28 fossils using several different sample sizes, n . We used fossil subsets of size $n = 4, 8, 12, 16, 20$, and 24. For each n , 20 fossil subsets were randomly chosen for divergence time analysis. Analyses were also performed using a single calibration ($n = 1$) for each of the 28 fossils. The same procedure was applied to each subsampled analysis. All subsampling analyses were performed using the method of Drummond and Rambaut (2007) and implemented in BEAST (Drummond and Rambaut 2007).

We compared the node age estimates for each subsampled analysis (148 total runs) against the estimates obtained from the 28-calibration analysis (herein referred to the “inclusive” analysis). For each of the internal nodes (194 total nodes), the posterior samples from the “subsampled” analysis were compared with the posterior from the “inclusive” analysis, resulting in 194 pairwise comparisons. We established five criteria to serve as a basis for our comparison: (i) Does the mean of the “subsampled” analysis fall within the 95% HPD interval of the “inclusive” analysis? (ii) Does the mean of the “inclusive” analysis fall within the 95% HPD interval of the “subsampled” analysis? (iii) Are the population means of the “inclusive” and “subsampled” distribution significantly different from each other? (iv) Does the 95% HPD interval of the “inclusive” and “subsampled” distributions overlap? (v) What is the distance between the “inclusive” and “subsampled” distributions? Criteria 1, 2, and 4 are easily determined by calculating the mean and 95% HPD interval of the node age distributions. Criterion 3 is calculated using a two-sample difference of means test; the estimates are significantly different from each other if 0 is not found within the 95% HPD interval. The fifth test, the two-sample Kolmogorov–Smirnov (K-S) test, is a non-parametric procedure for testing whether two samples were drawn from the same underlying continuous distribution. The K-S test statistic, D , is the maximum value of the absolute difference between two empirical distribution functions (EDFs). A value $D = 0$ indicates that the EDFs of the two samples are equal, while $D = 1$ implies the maximum difference between the two distributions. The P value of the test can be calculated using the Kolmogorov distribution as the null distribution. A schematic diagram of these performance criteria can be found in Figure 6.

Output from the MCMC chains was analyzed for convergence using the CODA package in R (Plummer et al. 2006). Parallel chains are considered to converge when the potential scale reduction factor (Gelman and Rubin 1992) is close to 1; the final 20 000 samples from each parallel chain are combined for further analysis. The effective sample size for each parameter is estimated to evaluate mixing.

RESULTS

Taxon Sampling and Model Selection

A total of 4 infraorders (100% coverage), 9 families (100% coverage), and 173 species from 79 genera within Achelata (100% genera coverage), Astacidea (95% generic coverage), Glypheidea (100% genera coverage), and Polychelida (66% generic coverage) were represented in all analyses (Supplementary Appendix S1; <http://dx.doi.org/10.5061/dryad.4v875>). A total of 184 12S sequences, 220 16S and 28S sequences, 223 18S sequences, 169 COI sequences, 206 H3 sequences, and 190 morphological characters were included in the combined phylogenetic analysis. The molecular data set (after GBLOCKS) totaled 4983 base pairs and the combined data set totaled 5173 characters. Duplicate species were excluded for the divergence time analysis and missing data were represented by “?” in the alignment. Phylogenetic reconstruction of the 10-partition scheme [by gene and codon {H3, COI}] did not differ statistically from the six-gene partitioned strategy (used in final analyses). Topology and bootstrap values were nearly identical with only minor differences at unsupported nodes between the two trees (10-partition vs. 6-partition). The best-fit model using the Bayesian Information Criterion (BIC) for the individual data set was a GTR model with invariant sites and γ -distribution (16S, COI), HKY model with invariant sites and γ -distribution (12S), TIMeF with invariant sites and γ -distribution (18S, 28S), and TVMef with invariant sites and γ -distribution (H3). A GTRCAT-based model was implemented in Phylobayes to compare against the GTRGAMMA model in RAxML. The effective sampling size for all parameters was >310 and the relative difference between chains for each parameter was 0–0.17 with the maximum difference between postburnin trees at 0.09. Many of the deeper relationships (infraorder level) could not be resolved in the GTRCAT model similar to that of the molecular only phylogeny (Supplementary Appendices S10 and S11; doi:10.5061/dryad.4v875). All infra orders were significantly supported and nearly all family-level, genus-level, and species-level relationships were identical to that of the molecular and combined total evidence phylogeny (see below). Most conflicting nodes were those that did not have high support in one or all of the analysis.

Phylogenetic Relationships

All individual gene and morphology trees are provided in the online Supplementary Appendices 4–8. A species tree was generated using iGTP and can also be found in the online Appendix S9 (doi:10.5061/dryad.4v875). The species tree recovers all infraorders and families to be monophyletic. A major difference in the species tree versus the concatenation approach is in the placement of *Cambaroides japonicus* (Appendices S9 and S10; doi:10.5061/dryad.4v875) and deep splits within Scyllaridae. However, most conflicting

nodes were those that did not have high support in one or all of the analysis.

Topologies and support values resulting from the combined and molecular analyses were highly congruent at the family, genus, and species levels. However, deep relationships (intra-infraordinal) were less resolved in the molecular phylogeny (Appendix S10; <http://dx.doi.org/10.5061/dryad.4v875>). Overall support across the tree increased with the addition of morphological evidence in the combined analysis (Fig. 3a,b). We recovered the lobster-like decapods as non-monophyletic (Fig. 3a,b). All families within lobster-like decapods were significantly supported as monophyletic (PP = 1 for Polychelidae, Palinuridae, Scyllaridae, Glypheidae, Enoplometopidae, Nephropidae, Astacidae, and Parastacidae) with the exception of Cambaridae with *Cambaroides japonicus* nesting within Astacidae (see “Discussion”). We recovered seven genera to be poly- or paraphyletic including *Polycheles*, *Petrarctus*, *Scyllarus*, *Acantharctus*, *Fallicambarus*, *Faxonella*, and *Procambarus*.

Lobster Divergence Time

All data were tested to assess if the individual data sets conformed to a strict molecular clock; a likelihood ratio test rejected the null hypothesis that the data followed a molecular clock ($P < 0.05$) for all individual gene data sets. All effective sample size (ESS) values were >200 for each individual run. Results from the empty alignment analysis showed that the fossil priors were not having a strong effect on our posterior divergence estimates.

Method 1: 28-fossil age analysis.—Runs were combined (40 000) in the final tree (Fig. 4). The origin of Decapoda was estimated in the Ordovician (~447 Ma, Fig. 4). Polychelids were the earliest lobster-like decapods to emerge (~372 Ma), with the most recent common ancestor of the present-day genera *Polycheles*, *Pentacheles*, *Willemoesia*, and *Stereomastis* placed within the Cretaceous (~99 Ma). Achelata diverged from the remaining Reptantia (=crawling lineages) around 357 Ma, with Palinuridae and Scyllaridae splitting from one another within the Permian (~254 Ma). The remaining lobster-like groups (Glypheidea and Astacidea) split from the other infraorders within the Carboniferous (~339 Ma) and quickly radiated into two separate lineages around ~318 Ma. Extant glypheid genera emerged only 24 Ma (*Laurentaeglyphea*, *Neoglyphea*). All five extant families within Astacidea arose throughout the Permian (~261 Ma: Parastacidae), Triassic (~222 Ma: Enoplometopidae, Nephropidae) and Jurassic (~161 Ma: Astacidae, Cambaridae). Northern hemisphere crayfish separated from the southern hemisphere crayfish around 261 Ma with subsequent family-level radiations of the northern hemisphere crayfish within the Jurassic.

Method 2: BPBP model.—The BPBP model estimates the origins of Decapoda to be 496 Ma with the earliest

TABLE 3. Comparison of the mean ages and highest posterior density/credible interval values across the four divergence dating methods for all major infraorders and families of lobster-like decapods

Divergence method	28-Fossil age model	BPBP model	Overlapping HPD intervals
Infraorders	Age (HPD)	Age (HPD)	
Polychelida	372.11 (354–399)	409.29 (385–451)	Yes
Achelata	357.41 (332–388)	391.27 (354–437)	Yes
Glypheidea	318.42 (287–349)	353.29 (318–390)	Yes
Astacidea	318.42 (287–349)	353.29 (318–390)	Yes
Family (MRCA)			
Polychelidae	99.64 (74–127)	89.97 (62–120)	Yes
Palinuridae	232.71 (199–263)	228.73 (186–269)	Yes
Scyllaridae	216.77 (186–247)	205.59 (167–243)	Yes
Glypheidae	24.6 (12–38)	22.74 (12–35)	Yes
Enoplometopidae	94.27 (58–134)	86.27 (53–123)	Yes
Nephropidae	181.3 (155–206)	156.09 (119–193)	Yes
Astacidae	151.85 (142–162)	84.02 (60–107)	No
Cambaridae	80.2 (71–90)	57.28 (44–69)	No
Parastacidae	215 (188–241)	205.29 (169–241)	Yes

branching lobster group, Polychelida, estimated to originate 409 Ma (Table 3 and Fig. 5). Achelata diverged soon thereafter ~391 Ma and the youngest lobster-like lineages, Glypheidea and Astacidea split from one another ~353 Ma (Table 3 and Fig. 5).

Fossil Calibration Subsampling Studies

Fossil subsampling.—Using a minimum threshold of 100 samples, all parameters of interest converged for all runs (see Methods). We compared all 148 runs from the subsampled analyses with the 28-calibration (fossil age) run (herein referred to as “inclusive” estimate/run). Each comparison involves 194 pairwise comparisons of the posterior distribution at each internal node. This amounts to over 28 000 nodes compared, each utilizing five different criteria (see Methods). Each node was color coded to indicate whether it satisfied each of the four yes/no criteria (Criteria 1–4, see Methods and Fig. 6). Node color corresponds to the number of criteria passed or failed by that particular node; “warmer” colors indicate that the node failed more criteria, whereas “cooler” colors imply that the subsampled estimate is closer to the 28-calibration estimate (“passed” our criteria) (Fig. 7). The overall trend in this table demonstrates that, with the addition of fossils, each run is converging closer to the “inclusive” estimate of divergence time (Fig. 7). In some instances, a single run did well with the addition of a few fossils (e.g., Fig. 7; run 12, 1-calibration point). Most nodes passed the four criteria once we added 12 fossils to the data set and nearly all nodes passed the criteria once 20 fossils were added. Twelve fossils represented ~42% of all fossils included in our “inclusive” analysis (=28 fossils), whereas 20 fossils represented ~71% of fossils included in our “inclusive” analysis. Our results indicate that some nodes (e.g., Fig. 7; 122, 123; 167, 168) performed poorly even with the

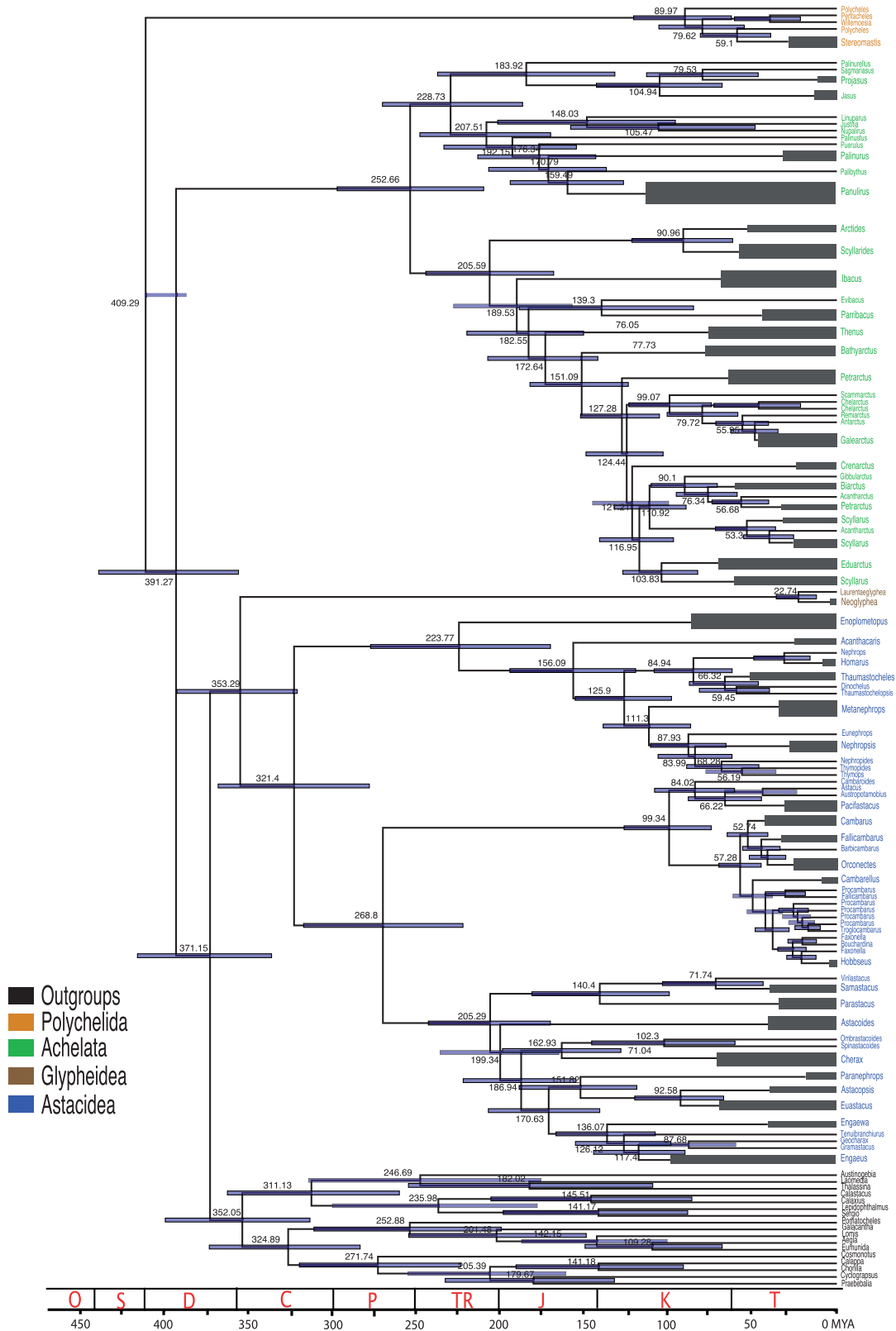
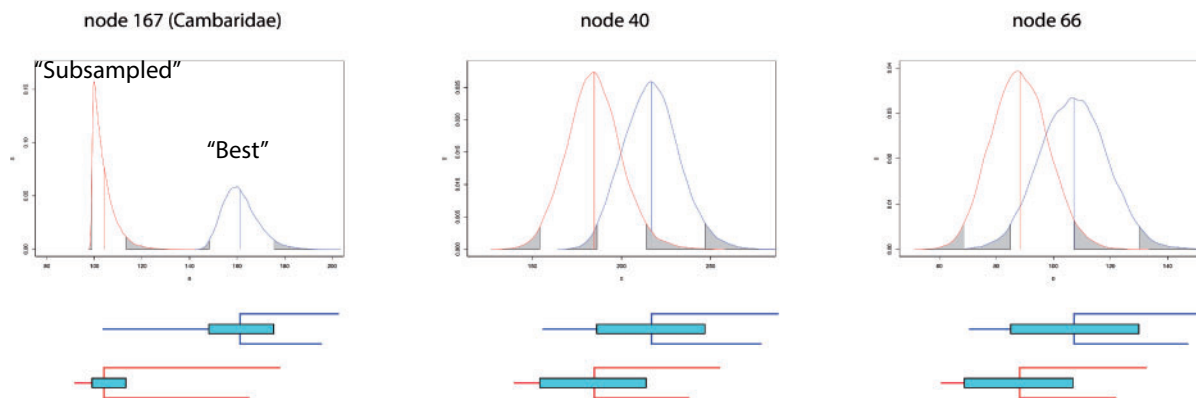


FIGURE 5. Divergence time chronogram using BPBP approach in BEAST. Divergence time estimates (Ma) are noted adjacent to their respective nodes and blue nodal bars correspond to the 95% highest posterior density regions. Geological periods are superimposed onto the phylogeny and listed as follows: O, Ordovician; S, Silurian; D, Devonian; C, Carboniferous; P, Permian; TR, Triassic; J, Jurassic; K, Cretaceous; T, Tertiary. Colored taxa correspond to the lobster-like decapod infraorders. Orange = Polychelida, Green = Achelata, Brown = Glypheidea, Blue = Astacidea.



Test	Node 167	Node 40	Node 66
Is subsampled mean within “inclusive” HPD?	NO	NO	YES
Is “inclusive” mean within subsampled HPD?	NO	NO	NO
Does subtracted distribution contain 0?	NO	YES	YES
Do HPD intervals overlap?	NO	YES	YES
K-S test statistic	1.00	0.71	0.62

FIGURE 6. Schematic example comparing the five performance criteria across three representative nodes.

TABLE 4. Summary statistics for the 5 performance criteria across all nodes given the sample size ($n = 1, 4, 8, 12, 16, 20, 24$ calibration/s)

Calibrations	Mean within “inclusive” HPD interval (min, max]	“Inclusive” mean within HPD interval (min, max)	Two-sample difference of means (min, max)	Overlapping HPD intervals (min, max)	Average K-S distance per node (min, max)	Percentage of nodes dated in tree (%)
1	26.9 (0, 91)	28.3 (0, 93)	43.3 (0, 94)	54.6 (0, 94)	0.800 (0.30, 1.00)	0.5
4	70.6 (13, 93)	73.8 (27, 96)	85.9 (57, 96)	92.2 (72, 98)	0.485 (0.22, 0.79)	2
8	68.1 (13, 93)	77.2 (36, 96)	84.8 (51, 96)	91.5 (70, 97)	0.471 (0.21, 0.80)	4
12	88.3 (54, 97)	91.8 (71, 99)	95.4 (78, 99)	97.0 (94, 99)	0.288 (0.13, 0.59)	6
16	89.1 (61, 97)	91.9 (73, 99)	95.4 (80, 99)	97.5 (94, 99)	0.286 (0.09, 0.55)	8
20	95.2 (76, 99)	96.2 (87, 100)	97.9 (95, 100)	98.5 (96, 100)	0.207 (0.07, 0.43)	10
24	98.2 (94, 100)	98.5 (88, 100)	99.3 (95, 100)	99.4 (96, 100)	0.151 (0.05, 0.37)	12

Note: For the first four statistics, the number indicates the average percentage of nodes that pass each test. The K-S test statistic measures whether the values sampled by each run are drawn from the same underlying distribution. In all cases, a higher KS number implies that the run is more different from the “inclusive.” The “min” and “max” represent the worst and best run for each n .

addition of fossils. In many instances, these nodes were clustered close to each other on the phylogeny.

Results were further condensed to illustrate the relative performance (i.e., the five criteria described

in fossil subsampling studies materials and methods) across all nodes, given the sample size (i.e., $n = 1, 4, 8, 12, 16, 20, 24$ calibration/s, Table 4). A single fossil calibration ($n = 1$) performed the worst when

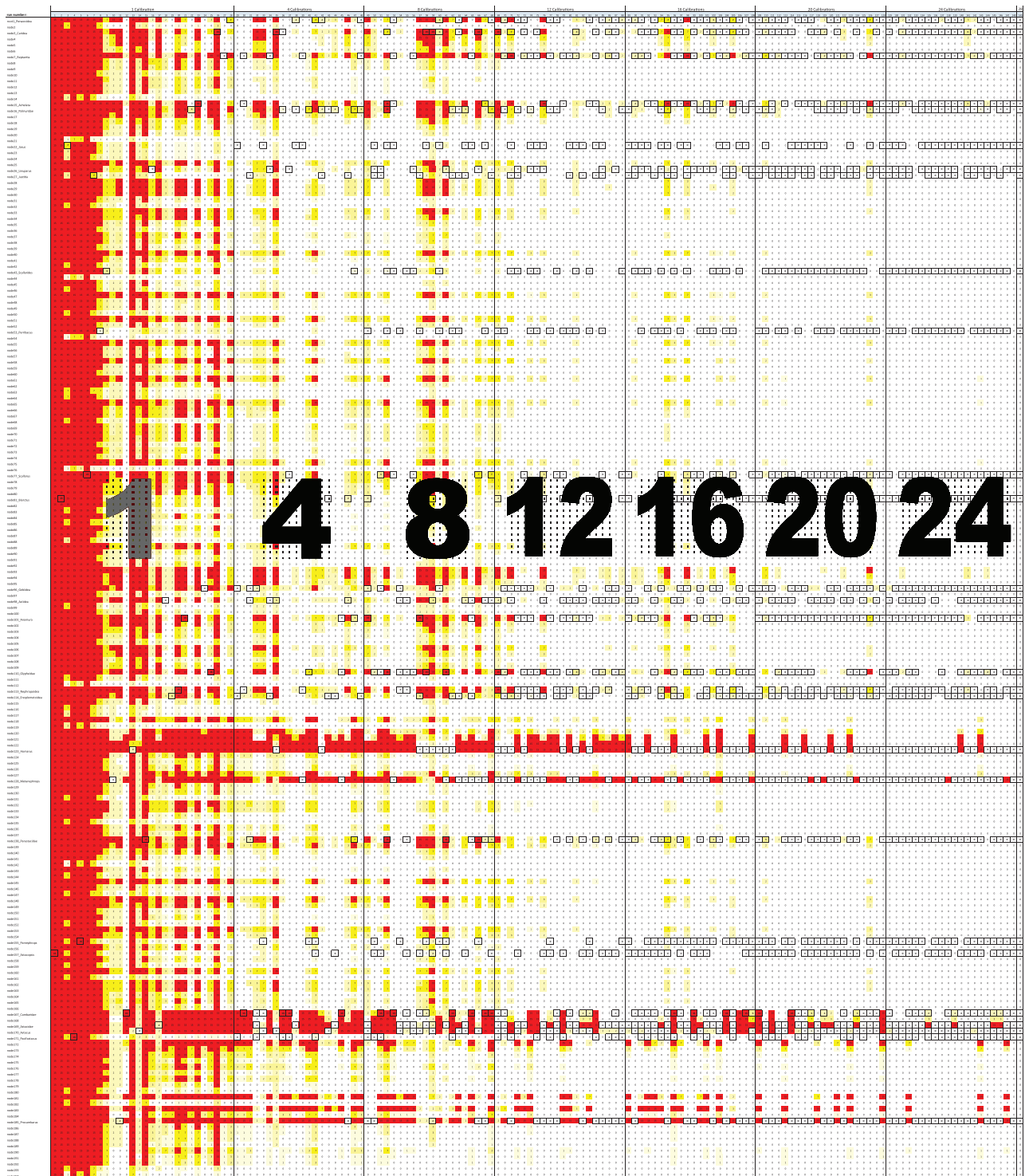


FIGURE 7. Graphical representation (heat matrix) of all fossil subsampling study results. All runs ($n = 149$) are sorted by number of calibrations (e.g., 1, 4, 8, 12, 24, 28). All nodes ($n = 194$) are assigned a success/failure score (coded by color) for each run. Each node was assigned a value between 0 and 4 according to whether that node passed (yes) or failed (no) the four performance criteria (#1–4) defined in the fossil subsampling materials and methods. Node color (red, bright yellow, pale yellow, and white) corresponds to the number of criteria passed or failed by that particular node (e.g., red = failed all four criteria, bright yellow = failed three, pale yellow = failed two, white = failed none). Boxed cells represent the priors included in the run.

compared to the “inclusive” estimate and had the largest variation (min, max) among runs. Increasing the number of calibrations from 4 to 8 did not seem to markedly change the relative performance of the divergence time estimations; however, 12 calibrations showed noticeable improvement over 8 calibrations. Similarly, an increase from 12 to 16 calibrations did not seem to notably impact the relative performance. The 20-calibration data set was >95% similar to the “inclusive” run with an average 0.207 K-S distance, whereas the 24-calibration was >98% similar to the “inclusive” run with a K-S distance of 0.151 (Table 4).

Dating Method Comparisons

Two methods that implemented different approaches for prior calibration (fossil age model vs. BPBP model) in BEAST were compared with test congruence of current methods. Compared to the 28-fossil age run, the BPBP model estimated slightly older divergence ages for all infraorders, but slightly younger ages (or near identical) for all families (Table 3 and Fig. 4, 5). All but two major clades (Astacidae and Cambaridae) had overlapping HPDs (Table 3).

DISCUSSION

Choice of Priors

Several studies have shown the choice of prior distributions and parameters have a direct effect on fossil calibration times (Lee and Skinner 2011; Lukoschek et al. 2012; Warnock et al. 2012); however, our study is the first to compare the effect of priors using a commonly used fossil age approach (Method 1: 28-fossil age analysis) and the novel approach of Wilkinson et al. (2011) (Method 2: BPBP approach). The prior distributions implemented in each approach varied (i.e., exponential vs. exponential/lognormal) and parameters were ultimately chosen depending on (i) the fit of the data, and/or (ii) a model of fossil discovery.

Overall, the 28-fossil and BPBP approaches showed increased concordance in divergence time estimates from deep (infraordinal) to shallow (family, genus) splits (Figs. 4 and 5). Estimates for most major lineages within lobster-like decapods are congruent with overlapping HPDs (see results, Table 3; Figs. 5 and 6). This result is particularly interesting considering the two methods utilize the fossil record very differently (see Methods) and increases our confidence in fossil assignment, selection, and final divergence estimates. As done herein, we suggest reporting the combined ages derived from all approaches when estimating divergence times for major lineages.

Estimates for two lobster families, Astacidae and Cambaridae, were not congruent across the fossil age and BPBP approach. The MRCA of Astacidae was estimated to be much older in the 28-fossil analysis when compared with the BPBP approach (151 Ma vs.

84 Ma). Based on fossil evidence, an astacid-like fossil, *Austropotamobius llopisi* Vía 1971, was discovered in the Kimmeridgian (~151–154 Ma), which was driving the age estimate in the 28-fossil age analysis. As fossil ages are not assigned to specific nodes, but rather incorporated as a model that uses species discovery through time in the BPBP approach, this node was estimated to be much younger (~84 Ma). The node that represents the MRCA of Cambaridae was also estimated to be younger in the BPBP analysis (80 Ma vs. 57 Ma, Table 3). One explanation for these drastically different estimates in the 28-fossil age analysis may be the interactions among priors on nearby branches to the node of interest (e.g., MRCA of Cambaridae) (see *Fossil Confidence and Interactions* below).

Fossil Calibration Subsampling Studies

In addition to testing prior choice on divergence estimates, we designed a fossil subsampling study to examine the effects of fossil density on divergence time estimates. We developed five criteria (see Methods) that allowed us to track the performance of the different fossil subsampling studies (Fig. 6). Our results suggest overlapping HPDs are the most conservative estimate with the alternate mean within the “inclusive” HPD interval being the most stringent (Table 4). Using the overlapping HPDs criteria, the inclusion of four calibration points resulted in 92% of the nodes appearing similar to the “inclusive” (28-fossil data set) run. In light of other performance tests, it becomes evident that the inclusion of four fossils may perform poorly when subject to more stringent performance criteria. For example, we see a steady decrease in performance (85.9%, 73.8%, 70.6%) when comparing the (i) 2-sample difference in means, (ii) “inclusive” mean within alternate HPD, and (iii) alternate mean with “inclusive” HPD, respectively (criteria 2–4, see Methods, Table 4). Although over 70% of the nodes in the 4-calibration run passed the most stringent performance criteria when compared with the “inclusive” run, an alarming result becomes evident when we take a closer look at the amount of variation associated with the performance criteria. As the performance criteria tests become more stringent, the amount of variation increases within runs (i.e., 20 runs for 1-calibration analysis), indicating that in many cases individual runs did much more poorly or better than our summary statistics report (Table 4). The largest amount of variation can be seen within the 1-fossil calibration runs, with the worst run (i.e., run 1) failing all four tests for all 194 nodes (Table 4; Fig. 7). In other words, the divergence time estimates for each node in this run showed no resemblance to our “inclusive” estimates, even under the most relaxed criteria (criteria 4, HPD overlap). On the contrary, several of the 1-calibration analyses performed very well; over 91% of the nodes in the best-performing 1-calibration (i.e., run 12) passed the most stringent test (Table 4, Fig. 7). Our results suggest

dating with 1-calibration on a data set of our magnitude (196 OTUs) is risky at best.

We were particularly interested in the following question: at what point does the addition of fossils only slightly affect our divergence time estimates? With the addition of fossils, accuracy improves (number of nodes that pass the criteria) and variation decreases, as expected (Table 4 and Fig. 7). However, when comparing performance across the table, it becomes clear that 4 and 8 calibrations yield similar results, as do 12 and 16 (Table 4). Although increasing the number of fossils may be a good strategy, these examples indicate some increases may result in similar performance and accuracy outcomes. It is important to note that the sheer number of fossils used in divergence dating analyses may not be as important as the proportion of fossil calibrations to OTUs. Our analysis contains 196 OTUs and with 28 fossil calibrations, allowing us to calibrate 14.4% of the nodes in the tree. Our results suggest only 10% of the nodes need to be calibrated (=20 fossils in our tree) to yield similar results (>95% similarity) to the “inclusive” estimate of divergence time (Table 4). Interestingly, a recent study by Erwin et al. (2011), which examined the effect of fossil calibration sampling on deep animal divergences, came to similar findings. In that study, they performed a 50% calibration-jack-knife analysis in which they repeatedly added 50% of their fossils at random (total number of fossils in analysis =24, each jack-knife analysis =12). Results indicated that deleting 50% of their calibration points did not significantly affect their divergence time estimates. A 50% reduction in fossils ($n = 12$) across the 124 OTUs used in their study is equivalent to dating 10% of the nodes in their tree. Based on our study and in accordance with Erwin et al. (2011), we recommend including at least 1 fossil per 10 OTUs in divergence dating analyses that use fossil calibrations. We do recognize that this recommendation will be dependent on quality and availability of the fossil record and degree of rate heterogeneity among taxa, all of which need to be considered in any divergence dating study.

The K-S test statistic has more power to differentiate among analyses by their relative performance. We have identified at least two factors that contribute to the discriminating power of this test. First, the K-S test uses the EDF of the posterior distribution, instead of point estimates (mean) and interval estimates (HPD interval) of the parameter value. Using sampled values from the posterior allows for [better] comparison between the underlying distributions. Second, the K-S test not only accounts for the location of the distribution, but is also sensitive to the shape of the distribution. Criteria 1–4 compare the locations of the “subsamped” and “inclusive” distributions while accounting for uncertainty using interval estimates. However, by only considering location, critical differences between estimates may be obscured. In this study, we found that the increased sensitivity of the K-S test provides a better understanding of the differences between and among different calibration sample sizes (Table 4). We witnessed

similar trends for the K-S test as we did for the other four performance criteria. The 4- and 8-calibration runs yield similar K-S distances and variation (min/max values) whereas the 12- and 16-calibration runs yield similar trends. The inclusion of 20- and 24-calibrations shows a progressive improvement in K-S distances and lower variation (Table 4).

Fossil Confidence and Interactions

Perhaps equally, if not more important, than the number (percentage) of calibrations in the tree, is the selection of priors and fossil confidence. All calibration points used in divergence time analyses should be based on age data (fossil and geological) generated from reliable sources. Fossils that cannot be assigned to a particular clade due to poor preservation or incompleteness of the fossil record should not be included. Fossil calibrations should only be used when they can be confidently assigned to a node on the tree for a fossil age approach. Likewise, for the BPBP approach, priors should only be constructed from fossils that can be assigned to a major lineage and geological age (i.e., epoch in our study) with associated extant species count data. Recently, detailed protocols for justifying fossil calibrations have been published (Parham et al. 2012). In many instances, calibration points were omitted from our phylogeny due to questionable nodal assignment.

The importance of fossil confidence and the selection of priors are evident in our fossil subsampling studies. Our results indicate that fossils interact dynamically with each other, and the removal or addition of any one fossil can have extreme effects on the divergence estimations (Fig. 7 and Table 4). It is apparent that certain regions of the tree performed relatively poorly in the majority of the subsampled runs (Fig. 7). One explanation for these “poor” nodal estimations could be interactions among the fossil calibration priors, because the sampled age for an ancestral node imposes a maximum bound (=upper bound) on the age of the descendant node. Alternatively, missing or absent calibrations on nearby nodes may allow the node to estimate an incorrect age. An example of this is within one of our 1-calibration runs (e.g., run 12, Fig. 7) where a mid-tree fossil, representing the family Cambaridae, estimated 195 of the 196 nodes correctly (when compared to the “inclusive” run). The only node estimated incorrectly was the calibration node itself. In this example, Cambaridae is directly affected by fossils above and below this node, which drive its divergence age estimate.

Fossil Placement

A secondary goal that emerged from the fossil subsampling study was to evaluate fossil placement (deep, middle, and shallow) on divergence time estimates. We looked closely at the 4-calibration subsampled runs in an attempt to identify patterns that

TABLE 5. The 20 runs from the 4-calibration analysis

Run	Performance criteria					Number of fossil priors			
	Mean within "inclusive" HPD	"Inclusive" mean within HPD interval	Two-sample difference of means	Overlapping HPD intervals	K-S test statistic	Sum	Deep	Middle	Shallow
run0038	23	7	7	5	41.9	83.9	1	1	2
run0043	24	11	8	7	46	96	0	2	2
run0039	14	16	11	11	53.1	105.1	1	1	2
run0044	32	13	7	4	61.2	117.2	0	2	2
run0045	15	19	12	11	68.9	125.9	0	3	1
run0037	18	21	14	12	77.3	142.3	0	1	3
run0042	46	14	13	5	70.5	148.5	1	1	2
run0029	27	34	16	13	83.5	173.5	0	2	2
run0036	36	46	16	13	90.4	201.4	1	2	1
run0030	39	51	16	13	91.5	210.5	2	2	0
run0034	39	57	16	13	94.8	219.8	1	2	1
run0048	40	64	16	13	97.5	230.5	2	2	0
run0031	56	57	20	13	104.5	250.5	0	3	1
run0046	77	42	22	14	101.8	256.8	0	1	3
run0040	65	91	41	16	120.8	333.8	0	2	2
run0032	104	55	47	16	119.2	341.2	0	2	2
run0047	82	110	54	19	129.1	394.1	0	3	1
run0033	131	64	53	17	132.2	397.2	0	1	3
run0041	106	141	75	34	144.7	500.7	1	0	3
run0035	168	104	84	54	152.7	562.7	1	1	2

Note: The number of calibrated nodes at each depth category (deep, middle, and shallow) is shown to demonstrate the effect of calibration placement. The numbers indicate the number of nodes (of 194) that passed the four performance criteria and the K-S test statistic. Overall performance was assessed by summing all statistics.

could predict relative performance. For example, if all calibration points are positioned at deep splits, will this have negative impacts (in performance) on shallow-level estimates? We partitioned the chronogram (deep, middle, and shallow; Fig. 4) and looked for correlations between the placement combinations (e.g., 3 shallow/1 middle; 3 middle/1 shallow; 1 deep/1 middle/2 shallow; 2 middle/2 shallow; Table 5). No clear pattern emerged relating placement combination to relative performance. Ironically, the best and worst runs from the 4-calibration study both contained 1 deep/1 middle/and 2 shallow fossils (Table 5). These results imply that correct age calibration and node assignment might have a larger impact on divergence time estimates than fossil depth placement (deep, middle, and shallow).

Finally, we examined not only the placement of fossils, but also the distribution (clustering) across the tree. In some instances (within the 4-calibration study), fossils that were clustered around a specific clade of the tree were ineffective in dating far-removed nodes. Although we could not extract a distinct trend, we suggest a wide distribution of fossil calibrations across breadth (i.e., across major lineages) and depth (deep, middle, and shallow) will allow for better divergence time estimations.

Although our preliminary results did not witness a trend in fossil placement studies, we acknowledge that our study only grazes the surface of potential factors contributing to placement and dating. Further studies with additional sample sizes, stratified subsampling of fossils according to depth and breadth, and non-random

placement of fossil calibrations are currently being explored to further examine this issue.

Evolutionary Relationships and Origins of Lobster-Like Decapods

Understanding phylogenetic relationships among and within lobster-like decapods is vital for unveiling the key factors responsible for their evolutionary success. For decades, the monophyly of lobster-like decapods has been under continuous debate. Much of the conflict comes from insufficient taxon sampling and alternative methods used to generate phylogenetic hypotheses (morphology vs. molecular data vs. combined). Owing to the rarity and inaccessibility of specimens of some taxa (i.e., Glypheidea), inclusion of all lobster lineages suitable for molecular and morphological analyses has been difficult. Furthermore, a dynamic classification has led to undersampling of major groups (i.e., Palinura = Achelata + Glypheidea + Polychelida). Past studies based on molecular and/or morphological data have found lobster-like decapods to be both monophyletic and non-monophyletic assemblages based on different genetic markers and evidence. In recent years, studies that have included all four infraorders based on morphological and molecular data have found lobsters to be non-monophyletic (Dixon et al. 2003; Ah Yong and Meally 2004; Bracken et al. 2009). However, molecular studies based on protein coding and ribosomal genes that have included three of the four infraorders have recovered a

monophyletic relationship between Astacidea, Achelata, and Polychelida (Tsang et al. 2008; Toon et al. 2009). Our current estimation of phylogenetic relationships based on six genes (mitochondrial and nuclear) and 190 morphological characters render the lobster-like decapods to be a non-monophyletic assemblage (Fig. 3a,b) in accordance with other studies based on total evidence (molecules and morphology).

Polychelida

Polychelids are commonly known as the deep-sea (exceeding 5000 m in *Willemoesia*, Galil 2000) blind lobsters due to the fact that all extant taxa possess reduced eyes and live in deep oceanic waters (Ahyong 2009). These lobsters are unique when compared with other reptant lineages in that all (five) or most (four) pairs of their legs are chelate. Present-day counts include 1 family, 6 genera, and 38 species with 3 families, 13 genera, and 55 species known as fossil representatives. Polychelids represent the oldest lobster lineage, dating back to the Devonian (~372/409 Ma, all dates reflect 28 fossil/BPBP approaches, Table 3; Figs. 4 and 5). Extinct fossil representatives differ most notably from present-day species in that many possessed well-developed eyes, suggesting a shallow water origin.

Achelata

Achelatans were the next to appear (~357/391 Ma), diverging into the two extant families, Palinuridae and Scyllaridae, around 250 Ma (Permian, Wuchiapingian). Achelata share numerous characters, most notably their phyllosoma larvae, that separate Achelata from all other Decapoda. In fact, the appearance of this specialized larval form may be traced back to the origin of achelatan, because fossil phyllosomas from the Upper Jurassic show that this type of larva has changed little in the last 200 million years (Polz 1971). Soon thereafter, Palinuridae split into two morphologically distinct lineages. *Limuparus*, *Justitia*, *Nupalirus*, *Palinustus*, *Puerulus*, *Palinurus*, *Palibythus*, and *Panulirus* form a clade known as the Stridentes, whereas *Projasus*, *Sagmariasus*, *Jasus* and the former synaxid genus *Palinurellus* form a clade known as the Silentes. The appearance of a stridulating organ, a complex sound-producing structure located on the antennal plate (found in Stridentes), may have provided these lobsters with advantages during predator escape (Lewis and Cane 1990), while expanding their communication abilities (Patek and Oakley 2003). Our phylogenetic analysis is consistent with the hypothesis that the stridulating organ provided Stridentes with an adaptive advantage promoting rapid diversification throughout the Jurassic (~200–160 Ma, Fig. 4). This time frame also coincides with the early break-up of Pangaea about 180 Ma. The ability to colonize new habitats during this event may have also facilitated the radiation and divergence of this group, as suggested in Astacidea (see below). Finally, the

main clades found within Scyllaridae are in agreement with current taxonomy based on adult morphology (Holthuis 1985, 1991, 2002) and recent molecular studies (Yang et al. 2011). Interestingly, the close relationship between *Parribacus* and *Evibacus* is also supported by larval morphology (Palero, unpublished results).

Glypheidea

Glypheid lobsters were presumed extinct since the Eocene (33.9–55.8 Ma). However, in 1908, a chance collection off the Philippines recovered a single male specimen that went unnoticed for almost seven decades until Forest and De Saint Laurent described it as *Neoglyphea inopinata* in 1975. Since its discovery, additional specimens have been collected from the opposite side of the Equator (Timor Sea) along with a new genus and species, *Laurentaeglyphea neocaledonica* (Richer de Forges 2006), from New Caledonia. Both living glypheid species (*Neoglyphea inopinata* and *Laurentaeglyphea neocaledonica*) are represented in our phylogeny. These two lineages appear to have evolved relatively recently, splitting from each other only 24/22 Ma (Oligocene, Chattian; Figs. 4 and 5).

Astacidea

Astacideans include the clawed lobsters and freshwater crayfish. They are divided into 4 superfamilies, 5 families, 44 genera, and 653 species. Our analysis includes all superfamilies, families, and 41 of the 44 genera. Higher level relationships have been well-resolved and well-documented within Astacidea (Crandall et al. 2000; Rode and Babcock 2003) and our results corroborate past findings. All families (Astacidae, Parastacidae, Enoplometopidae, and Nephropidae) are monophyletic with the exception of Cambaridae. The finding corroborates numerous morphological and molecular studies (Crandall et al. 2000; Rode and Babcock 2003; Porter et al. 2005; Braband et al. 2006; Bracken et al. 2009; Breinholt et al. 2009) and we conclude that *Cambaroides* should be included within Astacidae, as treated herein (Table 1 and Fig. 4). Additionally, the family-level status of Thaumastochelidae (*Thaumastochelodes*, *Thaumastochelopsis*, *Dinochelus*) has been variously supported (Dixon et al. 2003; Ahyong and Meally 2004; Schram and Dixon 2004) or challenged (Tsang et al. 2008) in previous analyses. Although our analysis supports the monophyly of the thaumastochelid group, they are deeply nested within Nephropidae and are best considered as derived nephropids.

Current hypotheses have speculated that northern hemisphere crayfish (Astacoidea) diverged from the southern hemisphere crayfish (Parastacoidea) ~200–185 Ma following the break-up of Pangaea (Crandall et al. 2000). Our results suggest this split may have commenced ~68–61 Ma earlier (261/268 Ma), and was later facilitated by the break-up of the supercontinent,

when several speciation events occurred within these lineages (~215–140 Ma). Interestingly, the 28-fossil run and BPBP approach converged on very similar mean values for this split (261/268 Ma). Our divergence time analysis is the first to not place a maximum age limit on this node, and without this constraint, we estimated an older age for this split when compared with previous studies (Porter et al. 2005; Breinholt et al. 2009; Bracken et al. 2010). Our results show that present-day southern hemisphere crayfish represent much older lineages when compared with their northern hemisphere counterparts. These older speciation events may have been facilitated by vicariance, resulting from the break-up of Gondwana in the early Jurassic (~176–201 Ma, although this conclusion has been recently confounded by the discovery of a parastacid crayfish in British Columbia dating to the Eocene (55 Ma) (Feldmann et al. 2011). This hypothesis is supported in previous studies (Toon et al. 2010) and our divergence time analysis that shows the early-branching South American crayfish clade splitting from the remaining southern hemisphere crayfish ~215/205 Ma. Present-day genera found on Madagascar (*Astacoides*) and New Zealand + Australia (sister clade to *Astacoides*) originated soon thereafter (~209/199 Ma).

SUPPLEMENTARY MATERIAL

Data available from the Dryad Digital Repository: <http://dx.doi.org/10.5061/dryad.4v875>.

FUNDING

This work was supported by the US National Science Foundation [EF-0531762, EF-0531603, EF-0531670], Research Fellowship Scheme of the Chinese University of Hong Kong [to L.M.T.]; the Research Grants Council of the Hong Kong Special Administrative Region [CUHK4419/04M to K.H.C.], the National Science Council and Academia Sinica [to T.Y.C.], and Brigham Young University [to K.A.C.].

ACKNOWLEDGMENTS

We acknowledge A. Crosnier, R. Cléva, and L. Corbari of the Muséum National d'Histoire Naturelle, Paris for providing many samples for the present molecular analysis. We also thank all other colleagues and institutions that have help with specimen collection, accompanied us on research cruises, and or provided advice/input to the preparation of this manuscript.

REFERENCES

Ahyong S.T. 2009. The polychelidan lobsters: phylogeny and systematics (Polychelida: Polychelidae). In: Martin J.W., Crandall

- K.A., Felder D.L., editors. Decapod crustacean phylogenetics. Boca Raton, FL: CRC Press (Crustacean issue 18), p. 360–390.
- Ahyong S., O' Meally D. 2004. Phylogeny of the Decapoda Reptantia: resolution using three molecular loci and morphology. *Raff. Bull. Zool.* 52:673–693.
- Apakupakul K., Siddall M.E., Bureson E.M. 1999. Higher level relationships of leeches (Annelida : Clitellata : Euhirudinea) based on morphology and gene sequences. *Mol. Phylogenet. Evol.* 12: 350–359.
- Azzalini A., Genton M.G. 2007. On Gauss's characterization of the normal distribution. *Bernoulli* 13:169–174.
- Battistuzzi F.U., Filipski A., Hedges S.B., Kumar S. 2010. Performance of Relaxed-Clock Methods in estimating evolutionary divergence times and their credibility intervals. *Mol. Biol. Evol.* 27:1289–1300.
- Bell, T. 1863. A monograph of the fossil malacostracous Crustacea of Great Britain, Pt. II, Crustacea of the Gault and Greensand. *Palaeontogr. Soc. Monogr.*, London:1–40, 11.
- Beschin C., De Angeli A., Garassino A. 2001. *Justitia vicetina* sp. nov. (Crustacea, Decapoda) dell'Eocene di Chiampo (Vicenza, Italia settentrionale). *Studi Trentini di Scienze Naturali, (Acta Geologica)* 76:89–97.
- Bohm J. 1922. Arthropoda. Crustacea. In: K. Martin (ed.), *Die Fossilien von Java. Sammlungen des Geologischen Reichsmuseums in Leiden, (neue Folge)* 1:521–535.
- Boisselier-Dubayle M., Bonillo C., Cruaud C., Couloux A., Richer de Forges B., Vidal N. 2010. The phylogenetic position of the "living fossils" Neoglypheia and Laurentaeglyhea (Decapod: Glypheidea). *C. R. Biol.* 333:755–759.
- Braband A., Kawai T., Scholtz G. 2006. The phylogenetic position of the East Asian freshwater crayfish *Cambaroides* within the Northern Hemisphere Astacoidea (Crustacea, Decapoda, Astacida) based on molecular data. *J. Zool. Sys. Evol. Res.* 44:17–24.
- Bracken H.D., De Grave S., Felder D.L. 2009. Phylogeny of the infraorder Caridea based on nuclear and mitochondrial genes (Crustacea: Decapoda). In: Martin J.W., Crandall K.A., Felder D.L., editors. Decapod crustacean phylogenetics. Boca Raton, FL: CRC Press (Crustacean issue 18), p. 274–300.
- Bracken H.D., Toon A., Felder D.L., Martin J.W., Finley M., Rasmussen J., Palero F., Crandall K.A. 2009. The Decapod tree of life: compiling the data and moving toward a consensus of decapod evolution. *Arthropod Syst. Phylogenet.* 67:99–116.
- Bracken H.D., De Grave S., Toon A., Felder D.L., Crandall K.A. 2010. Phylogenetic position, systematic status, and divergence time of the Procarididea (Crustacea: Decapoda). *Zool. Scripta* 39:198–212.
- Breinholt J., Pérez-Losada M., Crandall K.A. 2009. The timing of the diversification of the freshwater crayfishes. In: Martin J.W., Crandall K.A., Felder D.L., editors. Decapod crustacean phylogenetics. Boca Raton, FL: CRC Press (Crustacean issue 18), p. 305–318.
- Buhay J.E., Moni G., Mann N., Crandall K.A. 2007. Molecular taxonomy in the dark: Evolutionary history, phylogeography, and diversity of cave crayfish in the subgenus *Aviticambarus*, genus *Cambarus*. *Mol. Phylogenet. Evol.* 42:435–448.
- Castresana J. 2000. Selection of conserved blocks from multiple alignments for their use in phylogenetic analysis. *Mol. Biol. Evol.* 17:540–552.
- Chaudhary R., Bansal M.S., Wehe A., Fernandez-Baca D., Eulenstein O. 2010. iGTP: A software package for large-scale gene tree parsimony analysis. *BMC Bioinformatics* 11:574.
- Colgan D.J., McLauchlan A., Wilson G.D.F., Livingston S.P., Edgecombe G.D., Macaranas J., Cassis G., Gray M.R. 1998. Histone 3 and U2 snRNA DNA sequences and arthropod molecular evolution. *Aust. J. Zool.* 46:419–437.
- Cope E.D. 1871. On three extinct Astaci from the freshwater Tertiary of Idaho. *Proceedings of the American Philosophical Society* 11: 605–607.
- Crandall K.A., Fitzpatrick J.F. 1996. Crayfish molecular systematics: using a combination of procedures to estimate phylogeny. *Syst. Biol.* 45:1–26.
- Crandall K.A., Harris J.D., Fetzner J.W. 2000. The monophyletic origin of freshwater crayfish estimated from nuclear and mitochondrial DNA sequences. *Proc. R. Soc. Lond. Biol.* B 267:1679–1686.
- Dana J.D. 1852a. Parts I and II, Crustacea. U.S. Exploring Expedition During the Years 1838, 1839, 1840, 1841, 1842, under the Command

- of Charles Wilkes, U.S.N. Philadelphia: C. Sherman (1 map; separate folio atlas with 96 pls; Vol.13), p.1–1618.
- De Angeli A., Garassino A. 2008. *Pseudosquilla lessinea* n. sp. (Crustacea, Stomatopoda, Pseudosquillidae) and *Scyllarides bolcensis* n. sp. (Crustacea, Decapoda, Scyllaridae) from the Lower Eocene (Ypresian) of Monte Postale (Altissimo, Vicenza, NE Italy). *Atti della Società italiana di Scienze Naturali e del Museo civico di Storia naturale in Milano*, 149:167–178.
- De Grave S., Pentcheff N.D., Ah Yong S.T., Chan T.-Y., Crandall K.A., Dworschak P.C., Felder D.L., Feldman R.M., Franssen C., Goulding L. et al. 2009. A classification of living and fossil genera of decapod crustaceans. *Raff. Bull. Zool.* 21:1–109.
- Dixon C.J., Ah Yong S., Schram F.R. 2003. A new hypothesis of decapod phylogeny. *Crustaceana* 76:935–975.
- Drummond A.J., Ho S.Y.W., Phillips M.J., Rambaut A. 2006. Relaxed phylogenetics and dating with confidence. *PLoS Biol.* 4:699–710.
- Drummond A.J., Rambaut A. 2007. BEAST: Bayesian evolutionary analysis by sampling trees. *BMC Evol. Biol.* 7:214.
- Erwin D.H., Laflamme M., Tweedt S.M., Sperling E.A., Pisani D., Peterson K.J. 2011. The Cambrian conundrum: early divergence and later ecological success in the early history of animals. *Science* 334:1091–1097.
- Etallon A. 1861. Notes sur les Crustacés Jurassiques du bassin du Jura. *Mémoires de la Société de l'Agriculture, des Sciences et Lettres de la Haute Saône*, 9:129–171.
- Felder D.L., Robles R. 2009. Molecular phylogeny of the family Callianassidae based on preliminary analyses of two mitochondrial genes. In: Martin J.W., Crandall K.A., Felder D.L., editors. *Decapod crustacean phylogenetics*. Boca Raton, FL: CRC Press (Crustacean issue 18), p. 319–334.
- Feldmann R.M., Copeland M.J. 1988. A new species of erymid lobster from Lower Jurassic strata (Sinemurian/Pliensbachian), Fernie Formation, southwestern Alberta. *Contributions to Canadian Paleontology, Geological Survey of Canada, Bulletin* 379:93–101.
- Feldmann R.M., Pole M. 1994. A new species of *Paraneohrops* White, 1842: a fossil freshwater crayfish (Decapoda: Parastacidae) from the Manuherikia Group (Miocene), Central Otago, New Zealand. *New Zeal. J. Geol. Geop.* 37:163–167.
- Feldmann R.M., Schweitzer C.E. 2010. The oldest shrimp (Devonian: Fammenian) and remarkable preservation of soft tissue. *J. Crustacean Biol.* 30:629–635.
- Feldmann R.M., Schweitzer C.E., Leahy J. 2011. New Eocene crayfish from the Mcabee beds in British Columbia: First record of parastacoidea in the northern hemisphere. *J. Crust. Biol.* 31:320–331.
- Feldmann R.M., Schweitzer C.E., Hu S., Zhang Q., Zhou C., Xie T., Huang J., Wen W. 2012. Decapoda from the Luoping biota (Middle Triassic) of China. *J. Paleontol.* 86:425–441.
- Felsenstein J. 1985. Confidence-limits on phylogenies with a molecular clock. *Syst. Zool.* 34:152–161.
- Folmer O., Black M., Hoeh W., Lutz R., Vrijenhoek R. 1994. DNA primers for amplification of mitochondrial cytochrome c oxidase subunit I from diverse metazoan invertebrates. *Mol. Mar. Biol. Biotechnol.* 3:294–299.
- Forest J., de Saint Laurent M. 1975. Présence dans la faune actuelle d'un représentant du groupe mésozoïque des Glyphéides: *Neoglyphea inopinata* gen. nov., sp. nov. (Crustacea Decapoda Glypheidae). *Comptes Rendus Hebdomadaires de Séances de L'Académie des Sciences, Paris, (D)* 281:155–158.
- Forest J., de Saint Laurent M. 1976. Chace FA: *Neoglyphea inopinata*: A crustacean "living fossil" from the Philippines. *Science*, 192:884.
- Forster R., 1984. Bärenkrebse (Crustacea, Decapoda) aus dem Cenoman des Libanon und dem Eozän Italiens. *Mitteilungen der Bayerischen Staatssammlung für Paläontologie und Historische Geologie* 24: 57–66.
- Garassino A., Teruzzi G. 1993. A new decapod crustacean assemblage from the Upper Triassic of Lombardy (N. Italy). *Paleontologia Lombarda, (nuova serie)* 1:1–27.
- Gelman A., Rubin D.B. 1992. Inference from iterative simulation using multiple sequences. *Stat. Sci.* 7:457–511.
- Glaessner M.F. 1960. The fossil decapod Crustacea of New Zealand and the evolution of the order Decapoda. *New Zeal. Geol. Surv. Paleontol. Bull.* 31:3–63.
- Gray J.E., 1845. Description of some new Australian animals. In: Edward John Eyre, *Journals of Expeditions of Discovery into Central Australia, etc.*, 1:405–411.
- Ho S.Y.W. 2007. Calibrating molecular estimates of substitution rates and divergence times in birds. *J. Avian Biol.* 38:409–414.
- Ho S.Y.W. 2009. An examination of phylogenetic models of substitution rate variation among lineages. *Biol. Lett.* 5:421–424.
- Holthuis L. 1985. A revision of the family Scyllaridae (Crustacea: Decapoda: Macrura). I. Subfamily Ibacininae. *Zool. Verhandl.* 218: 1–130.
- Holthuis L. 2002. The Indo-Pacific scyllarine lobsters (Crustacea, Decapoda, Scyllaridae). *Zoosystema* 24:499–683.
- Holthuis L.B. 1991. Marine lobsters of the world. An annotated and illustrated catalogue of species of interest to fisheries known to date. Rome: Food and Agriculture Organization of the United Nations (FAO species catalog; vol. 13).
- Huelsenbeck J.P., Ronquist F. 2001. MrBAYES: Bayesian inference of phylogeny. *Biometrics* 17:754–755.
- Inoue J., Donoghue P.C.J., Yang Z.H. 2010. The impact of the representation of fossil calibrations on Bayesian estimation of species divergence times. *Syst. Biol.* 59:74–89.
- Jones J.P.G., Andriahajaina F.B., Ranambintsoa E.H., Hockley N.J., Ravoahangimalala O. 2006. The economic importance of freshwater crayfish harvesting in Madagascar and the potential of community-based conservation to improve management. *Oryx* 40:168–175.
- Karasawa H., Schweitzer C.E., Feldmann R.M. 2013. Phylogeny and systematics of extant and extinct lobsters. *J. Crust. Biol.* 33:78–123.
- Lanfear R., Calcott B., Ho S.Y.W., Guindon S. 2012. PartitionFinder: combined selection of partitioning schemes and substitution models for phylogenetic analyses. *Mol. Biol. Evol.* 29:1695–1701.
- Lartillot N., Lepage T., Blanquart S. 2009. PhyloBayes 3: a Bayesian software package for phylogenetic reconstruction and molecular dating. *Bioinformatics* 25:2286–2288.
- Lartillot N., Philippe H. 2004. A Bayesian mixture model for across-site heterogeneities in the amino-acid replacement process. *Mol. Biol. Evol.* 21:1095–1109.
- Lee M.S.Y., Skinner A. 2011. Testing fossil calibrations for vertebrate molecular trees. *Zool. Scr.* 40:538–543.
- Lepage T., Bryant D., Philippe H., Lartillot N. 2007. A general comparison of relaxed molecular clock models. *Mol. Biol. Evol.* 24:2669–2680.
- Lewis P.O. 2001. A likelihood approach to estimating phylogeny from discrete morphological character data. *Syst. Biol.* 50:913–925.
- Lewis E.E., Cane J.H. 1990. Stridulation as a primary antipredator defense of a beetle. *Anim. Behav.* 40:1003–1004.
- Lukoschek V., Keogh J.S., Avise J.C. 2012. Evaluating fossil calibrations for dating phylogenies in light of rates of molecular evolution: A comparison of three approaches. *Syst. Biol.* 61:22–43.
- Maddison W.P., Maddison D.R. 2010. Mesquite: a modular system for evolutionary analysis. Version 2.73. Available from: <http://mesquiteproject.org>.
- Martin A.J., Austin C.M., Kool L., Poore G.C.B., Rich T.H., Schultz M.B., Vickers-Rich P. 2008. Fossil evidence in Australia for oldest known fresh-water crayfish of Gondwana. *Gondwana Res.* 14:287–296.
- Medlin L.K., Elwood H.J., Stickel S., Sogin M.L. 1988. The characterization of enzymatically amplified eukaryotic 18S-like rRNA coding regions. *Gene* 71:491–499.
- Packard A.S. 1880. Fossil crawfish from the tertiaries of Wyoming. *Am. Nat.* 14:222–223.
- Palero F., Guerao G., Clark P.F., Abelló P. 2008. The true identities of the slipper lobsters *Nisto laevis* and *Nisto asper* (Crustacea: Decapoda: Scyllaridae) verified by DNA analysis. *Invertebr. Syst.* 23:77–85.
- Parham J., Donoghue P., Bell C., Calway T., Head J., Holroyd P., Inou J., Irmis R., Joyce W.G., Ksepka D.T., Patané J.S.L., Smith N.D., Tarver J.E., Van Tuinen M., Yang Z., Angielczyk K.D., Greenwood J., Hipsley C.A., Jacobs L., Makovicky P.J., Müller J., Smith K.T., Theodor J.M., Warnock R.C.M., Benton M.J. 2012. Best practices for justifying fossil calibrations. *Syst. Biol.* 61:346–359.
- Patek S.N., Oakley T.H. 2003. Comparative tests of evolutionary trade-offs in a palinurid lobster acoustic system. *Evolution* 57: 2082–2100.
- Perez-Losada M., Hoeg J.T., Crandall K.A. 2004. Unraveling the evolutionary radiation of the thoracican barnacles using molecular

- and morphological evidence: a comparison of several divergence time estimation approaches. *Syst. Biol.* 53:244–264.
- Pinna G. 1974. I crostacei della fauna triassica di Cene in Val Seriana (Bergamo). *Memorie della Società italiana di Scienze naturali e del Museo civico di Storia naturale in Milano* 21:5–34.
- Plummer M., Best N., Cowles K. 2006. CODA: Convergence diagnosis and output analysis for MCMC. *R. News* 6:7–11.
- Polz H. 1971. Eine weitere Phyllosoma-Larve aus den Solnhofener Plattenkalken. *Neues Jahrbuch für Geologie und Paläontologie. Monatshefte* 8:474–488.
- Porter M.L., Perez-Losada M., Crandall K.A. 2005. Model-based multi-locus estimation of decapod phylogeny and divergence times. *Mol. Phylogenet. Evol.* 37:355–369.
- Posada D., Crandall K.A. 1998. MODELTEST: testing the model of DNA substitution. *Bioinformatics* 14:817–818.
- Rambaut A., Drummond A.J. 2007. Tracer v1.4. Available from: <http://beast.bio.ed.ac.uk/Tracer>.
- Reed F.R.C. 1911. New Crustacea from the Lower Greensand of the Isle of Wight. *Geol. Mag.* 8:115–120.
- Richer de Forges B. 2006. Découverte en mer du Corail d'une deuxième espèce de glyphéide (Crustacea, Decapoda, Glypheoidea). *Zoosystema* 28:17–29.
- Robles R., Tudge C.C., Dworschak P.C., Poore G.C.B., Felder D.L. 2009. Molecular phylogeny of the Thalassinidea based on nuclear and mitochondrial genes. In: Martin J.W., Crandall K.A., Felder D.L., editors. *Decapod crustacean phylogenetics*. Boca Raton, FL: CRC Press (Crustacean issue 18), p. 301–318.
- Rode A.L., Babcock L.E. 2003. Phylogeny of fossil and extant freshwater crayfish and some closely related nephropid lobsters. *J. Crust. Biol.* 23:418–435.
- Ronquist F., Klopfstein S., Vilhelmsen L., Schulmeister S., Murray D.L., Rasnitsyn A.P. 2012. A total-evidence approach to dating with fossils, applied to the early radiation of the Hymenoptera. *Syst. Biol.* 61:973–999.
- Rutschmann F., Eriksson T., Abu Salim K., Conti E. 2007. Assessing calibration uncertainty in molecular dating: the assignment of fossils to alternative calibration points. *Syst. Biol.* 56:591–608.
- Sanderson M.J. 2003. r8s: inferring absolute rates of molecular evolution and divergence times in the absence of a molecular clock. *Bioinformatics* 19:301–302.
- Scholtz G., Richter S. 1995. Phylogenetic systematics of the reptantian Decapoda (Crustacea, Malacostraca). *Zool. J. Linn. Soc.-Lond.* 113:289–328.
- Schram, F. R., 1971. *Litogaster turnbullensis*, a Lower Triassic glypheid decapod crustacean from Idaho. *J. Paleo.* 45:534–537.
- Schram F.R., Dixon C.J. 2004. Decapod phylogeny: addition of fossil evidence to a robust morphological cladistic data set. *Bull. Mitunami Fossil Museum* 31:1–19.
- Schram F.R., Feldmann R.M., Copeland M.J. 1978. The late Devonian Palaeopalaemonidae and the earliest decapod crustaceans. *J. Palaeo.* 52:1375–1387.
- Schwarz G. 1978. Estimating the dimensions of a model. *Ann. Stat.* 6:461–464.
- Schweigert G., Garassino A., Hall L.R., Hauff R.B., Karasawa H. 2003. The lobster genus *Uncina* Quenstedt, 1851 (Crustacea: Decapoda: Astacidea: Uncinidae) from the Lower Jurassic. *Stuttgarter Beiträge zur Naturkunde, (B)* 332:1–43.
- Schweitzer C., Feldmann R., Garassino A., Karasawa H., Schweigert G. 2010. Systematic list of fossil decapod crustacean species, crustaceana monographs. Leiden, Boston: Brill.
- Song H., Buhay J.E., Whiting M.F., Crandall K.A. 2008. Many species in one: DNA barcoding overestimates the number of species when nuclear mitochondrial pseudogenes are coamplified. *Proc. Natl Acad. Sci. USA.* 105:13486–13491.
- Stamatakis A., Blagojevic F., Nikolopoulos D.S., Antonopoulos C.D. 2007. Exploring new search algorithms and hardware for phylogenetics: RAXML meets the IBM cell. *J. VLSI Signal Proc.* 48:271–286.
- Stamatakis A., Hoover P., Rougemont J. 2008. A rapid bootstrap algorithm for the RAXML web servers. *Syst. Biol.* 57:758–771.
- Stamatakis A., Ludwig T., Meier H. 2005. RAXML-III: A fast program for maximum likelihood-based inference of large phylogenetic trees. *Bioinformatics* 21:456–463.
- Steneck R.S., Hughes T.P., Cinner J.E., Adger W.N., Arnold S.N., Berkes F., Boudreau S.A., Brown K., Folke C., Gunderson L., Olsson P., Scheffer M., Stephenson E., Walker B., Wilson J., Worm B. 2011. Creation of a gilded trap by the high economic value of the Maine Lobster Fishery. *Conserv. Biol.* 25:904–912.
- Stenzel H.B. 1945. Decapod crustaceans from the Cretaceous of Texas. The University of Texas Publication 4401:401–477.
- Swahn J.O. 2004. The cultural history of crayfish. *Bull. Fr. Peche Piscic.* 372–373:243–251.
- Talavera G., Castresana J. 2007. Improvement of phylogenies after removing divergent and ambiguously aligned blocks from protein sequence alignments. *Syst. Biol.* 56:564–577.
- Toon A., Finley M., Staples J., Crandall K.A. 2009. Decapod phylogenetics and molecular evolution. In: Martin J.W., Crandall K.A., Felder D.L., editors. *Decapod crustacean phylogenetics*. Boca Raton, FL: CRC Press (Crustacean issue 18), p. 14–28.
- Toon A., Perez-Losada M., Schweitzer C.E., Feldmann R.M., Carlson M., Crandall K.A. 2010. Gondwanan radiation of the Southern Hemisphere crayfishes (Decapoda: Parastacidae): evidence from fossils and molecules. *J. Biogeogr.* 37:2275–2290.
- Tsang L.M., Ma K.Y., Ah Yong S.T., Chan T.Y., Chu K.H. 2008. Phylogeny of Decapoda using two nuclear protein-coding genes: origin and evolution of the Reptantia. *Mol. Phylogenet. Evol.* 48:359–368.
- Van Straelen V. 1925. Contribution à l'étude des Crustacés Décapodes de la période jurassique. *Mémoires d'Académie Royale de Belgique, (Science)*, 7:1–462.
- Van Straelen, V. 1928c. On a fossil freshwater crayfish from eastern Mongolia. *Bulletin of the Geological Society of China, Peking*, 7:133–138.
- Von Meyer H. 1834. *Krebse im bunten Sandstein*. Museum Senckenbergianum 1:293–295.
- Walker J.D., Geissman J.W. 2009. Geologic time scale: Geological Society of America. Boulder, CO The Geological Society of America doi: 10.1130/1052-5173-19.4-5.60.
- Warnock R.C.M., Yang Z.H., Donoghue P.C.J. 2012. Exploring uncertainty in the calibration of the molecular clock. *Biol. Lett.* 8:156–159.
- Whitfield R.P. 1880. Notice of new forms of fossil crustaceans from the Upper Devonian rocks of Ohio, with descriptions of new genera and species. *Am. J. Sci.* 19:33–42.
- Whiting M.F. 2002. Mecoptera is paraphyletic: multiple genes and phylogeny of Mecoptera and Siphonaptera. *Zool. Scr.* 31: 93–104.
- Whiting M.F., Carpenter J.C., Wheeler Q.D., Wheeler W.C. 1997. The strepsiptera problem: phylogeny of the holometabolous insect orders inferred from 18S and 28S ribosomal DNA sequences and morphology. *Syst. Biol.* 46:1–68.
- Wilkinson R.D., Steiper M., Soligo C., Martin R., Yang Z., Tavaré S. 2011. Dating primate divergences through an integrated analysis of palaeontological and molecular data. *Syst. Biol.* 60: 16–31.
- Wilkinson R.D., Tavaré S. 2009. Estimating primate divergence times by using conditioned birth-and-death processes. *Theor. Popul. Biol.* 75:278–285.
- Yang C.H., Bracken-Grissom, H., Kim D., Crandall K.A., Chan T.-Y. 2011. Phylogenetic relationships, character evolution, and taxonomic implications within the slipper lobsters (Crustacea: Decapoda: Scyllaridae). *Mol. Phylogenet. Evol.* 62:237–250.